



Signatures of Space Weather events in low latitudes ionosphere quiet and disturbed magnetic periods

Christine Amory-Mazaudier

LPP, CNRS/Ecole Polytechnique/Sorbonne Université/Université Paris-Sud/Observatoire de Paris

christine.amory@lpp.polytechnique.fr

African Capacity building workshop on space weather effects on GNSS, Trieste 3 -14 October 2022

Outline

- Introduction
- Characteristics of the low latitudes
Equatorial Fountain, Pre Reversal Enhancement, Equatorial electrojet
- Plasma irregularities
ROTI-S4
- Variations of ionospheric parameters due to solar electromagnetic emissions
Total electron content TEC, Earth's magnetic field variations
- Electrodynamical coupling between high and low latitudes
TEC, ROTI, Earth's magnetic field variations
- Conclusion

IMPACT on Technologies

The ionosphere is a ionized layer around the Earth (from ~ 50 km up to 800 km).
Ionospheric electric currents are at the origin of variations of the Earth's magnetic field and Ground Induced Electric Currents (GIC)

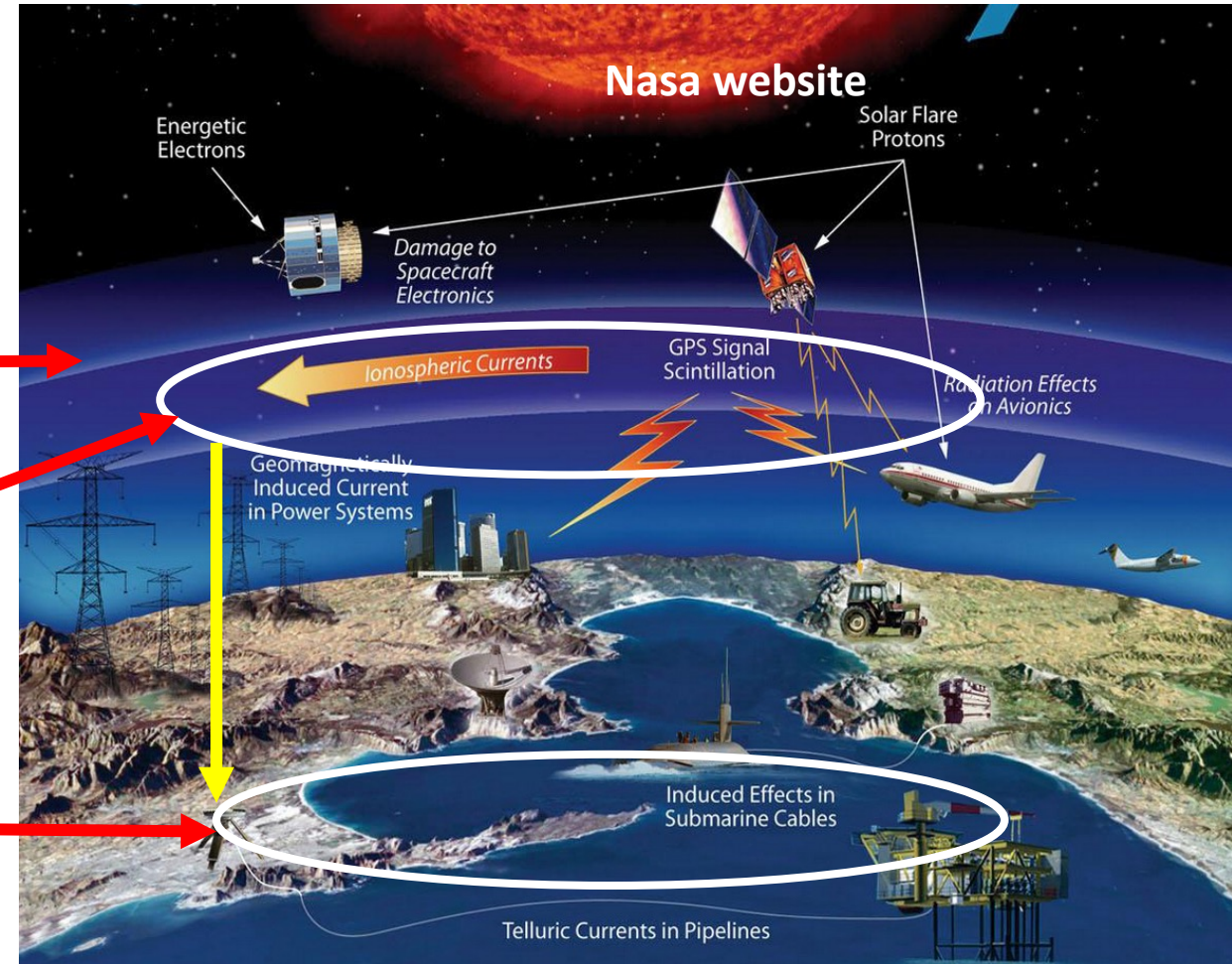
Regular and irregular variations

1 Ionization

Propagation of electromagnetic waves

2) Ionospheric electric current

3) Variations of the Earth's magnetic field and GIC



Outline

- Introduction

- **Characteristics of the low latitudes**

Equatorial Fountain, Pre Reversal Enhancement, Equatorial electrojet

- Plasma irregularities

ROTI-S4

- Variations of ionospheric parameters due to solar electromagnetic emissions

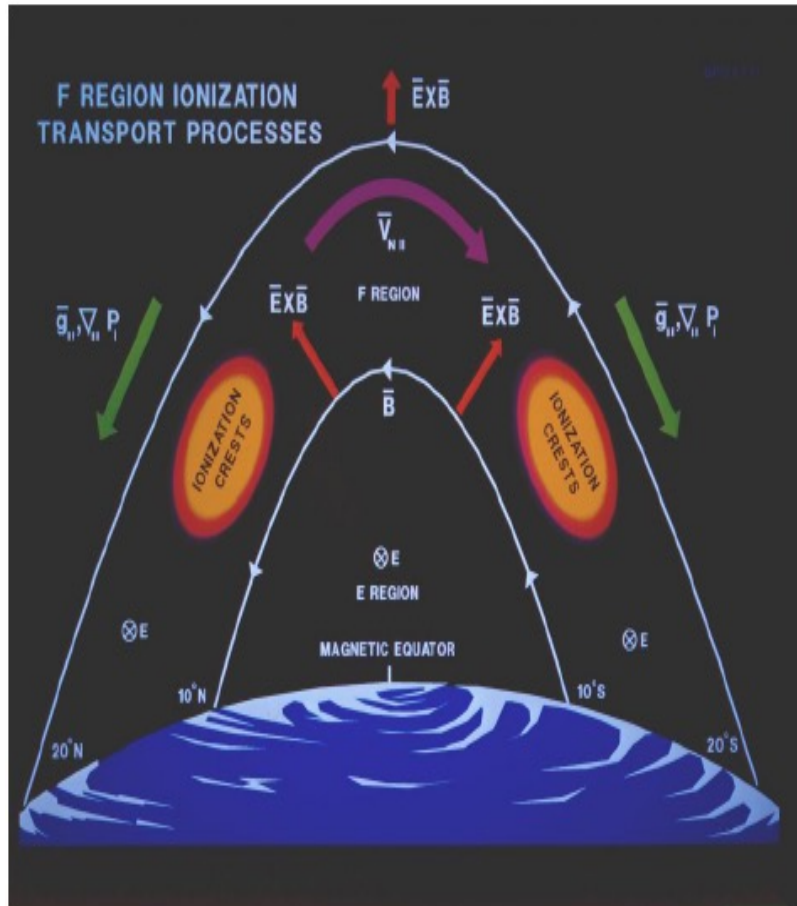
Total electron content TEC, Earth's magnetic field variations

- Electrodynamical coupling between high and low latitudes

TEC, ROTI, Earth's magnetic field variations

- Conclusion

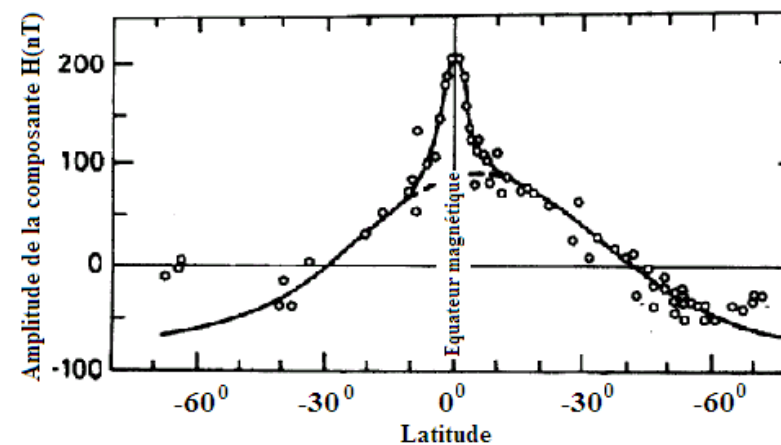
PHYSICS of Low latitudes



Equatorial Fountain

Eastward electric field => moves up
Westward electric field => moves down

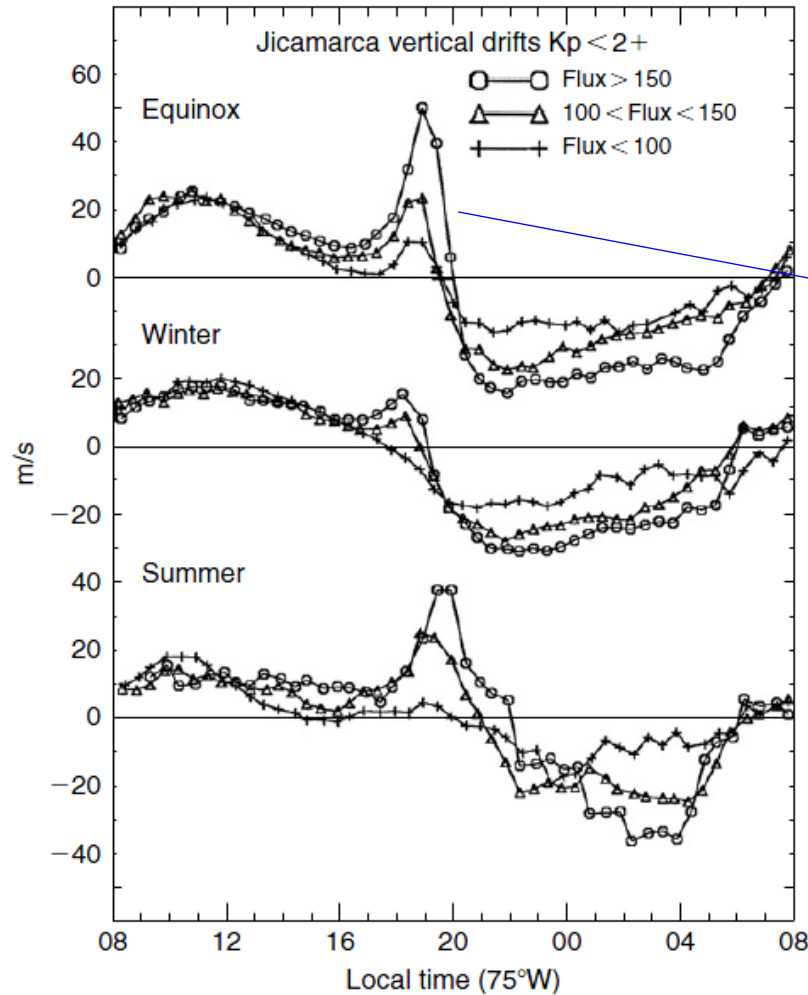
At equator the Earth's magnetic field is horizontal
During the daytime the east–west electric field and the north–south geomagnetic field produce the lift of plasma in E ionospheric region by **vertical $E \times B$ drift**.
At higher altitudes in F region, the plasma diffuses downward along the geomagnetic field lines into both hemispheres under the influence of gravity and pressure gradients, this produces the EIA which is characterized by an electron density trough at the magnetic equator, and two crests of enhanced electron density at about $\pm 15^\circ$ magnetic latitude



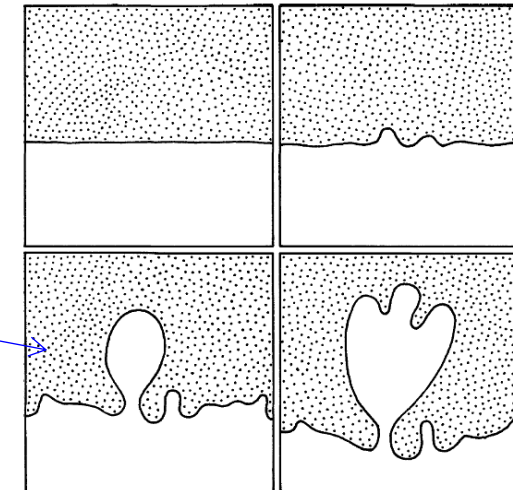
The Equatorial Electrojet (Jacobs, 1990)

PRE : Pre Reversal Enhancement

Equatorial Plasma Bubbles



Magnetic quiet time



Sequential diagram, from photos, of the development of a Rayleigh Taylor instability. The heaviest fluid [... ..], over a lighter and more transparent fluid
Kelley, M.C., (1989), the Earth Ionosphere, ed. Academic Press, San Diego.

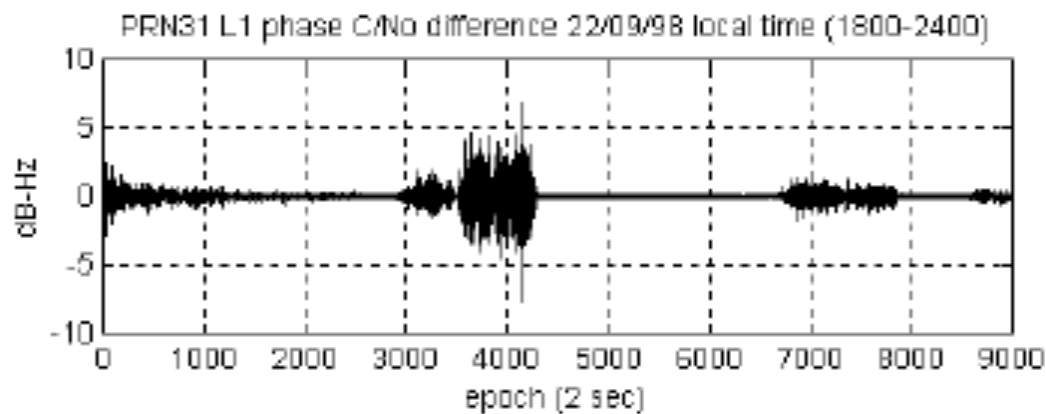
Average vertical plasma velocities at Jicamarca during the equinox (March-April, September-October), winter (May-August), summer (November-February) for 3 solar flux values
Fejer, et al., Average vertical and zonal F region drifts over Jicamarca, Journal of Geophys. Res, Vol. 96, N° A8, page 13901-13906, 1991

Ionospheric propagation

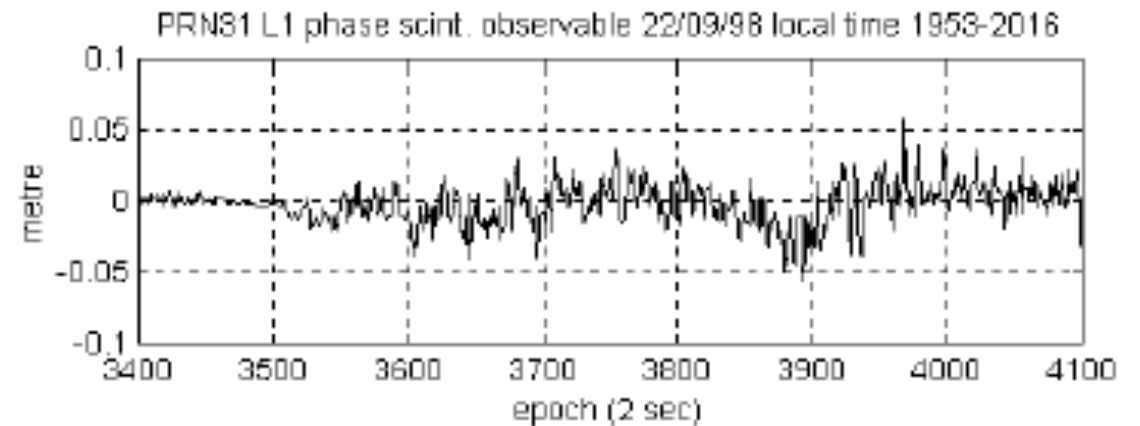
Scintillations

Fluctuations of the signal due to the inhomogeneity of the medium as plasma bubbles

Scintillations of amplitude



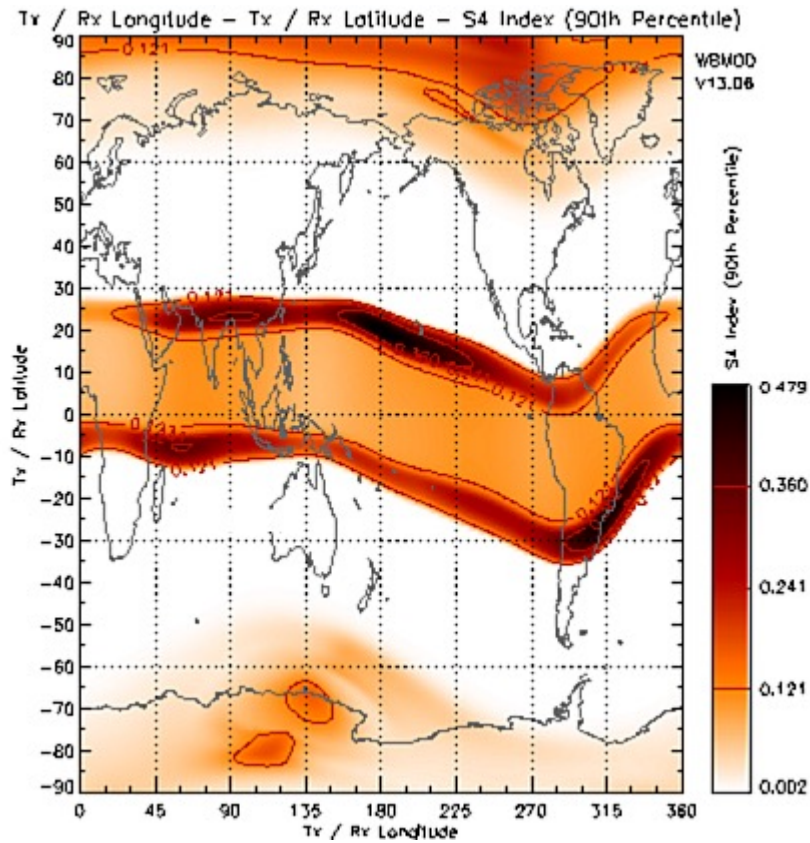
Scintillations of phase



scales : ± 3 rad.

Scintillations a regular phenomenon

Ionospheric scintillation is the rapid modification of radio waves caused by small scale structures in the ionosphere, **Physical Process : Instabilities in Plasma**



Indice of scintillation $s4 = \sqrt{\frac{\langle I^2 \rangle - \langle I \rangle^2}{\langle I \rangle^2}}$

Scintillation index at GPS L1 (1575.42 MHz)
assuming constant local time 23.00 at all longitudes
(from <http://www.sws.bom.gov.au>)

“Ionospheric scintillation is primarily an equatorial and high-latitude ionospheric phenomenon, although it can (and does) occur at lower intensity at all latitudes. Ionospheric scintillation generally peaks in the sub-equatorial anomaly regions, located on average $\sim 15^\circ$ either side of the geomagnetic equator.”

Outline

- Introduction
- Characteristics of the low latitudes

Equatorial Fountain, Pre Reversal Enhancement, Equatorial electrojet

- **Plasma irregularities**

ROTI-S4

- Variations of ionospheric parameters due to solar electromagnetic emissions

Total electron content TEC, Earth's magnetic field variations

- Electrodynamical coupling between high and low latitudes

TEC, ROTI, Earth's magnetic field variations

- Conclusion

PLASMA IRREGULARITIES

S4 -> fluctuations of the GPS power signal

$$I = \frac{A^2}{2}$$

$$s4 = \sqrt{\frac{\langle I^2 \rangle - \langle I \rangle^2}{\langle I \rangle^2}}$$

ROTI Index

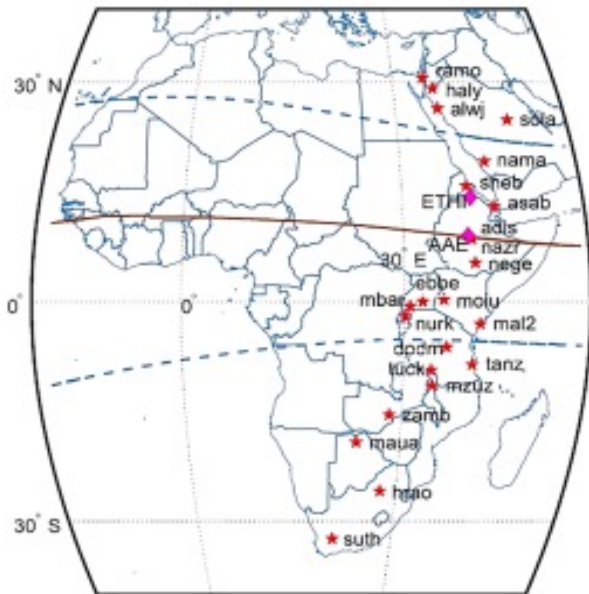
$$\text{rot} = \frac{STEC_{k+1} - STEC_k}{time_{k+1} - time_k} * 60$$

$$\text{roti} = \sqrt{\langle \text{rot}^2 \rangle - \langle \text{rot} \rangle^2}$$

Training on daily global positioning system GPS data , Coordinates a monthly magazine on positioning, navigation and beyond, <http://www.mycoordinates.org>, **Volume XIII, Issue 03, March 2017** (Amory-Mazaudier, Rolland Fleury, Sharafat Gadimova, Abderrahmane Touzani)
Software of Rolland Fleury on www.girgea.org

Quiet-time ionospheric irregularities over the African Equatorial Ionization Anomaly (EIA) Region on April 9th 2013,

Amaechi et al., Radio Science, 55, e2020RS007077. <https://doi.org/10.1029/2020RS007077>



- Magnetic equator
- - - ± 15° dip latitude
- ★ GNSS station
- ◆ Magnetometer station

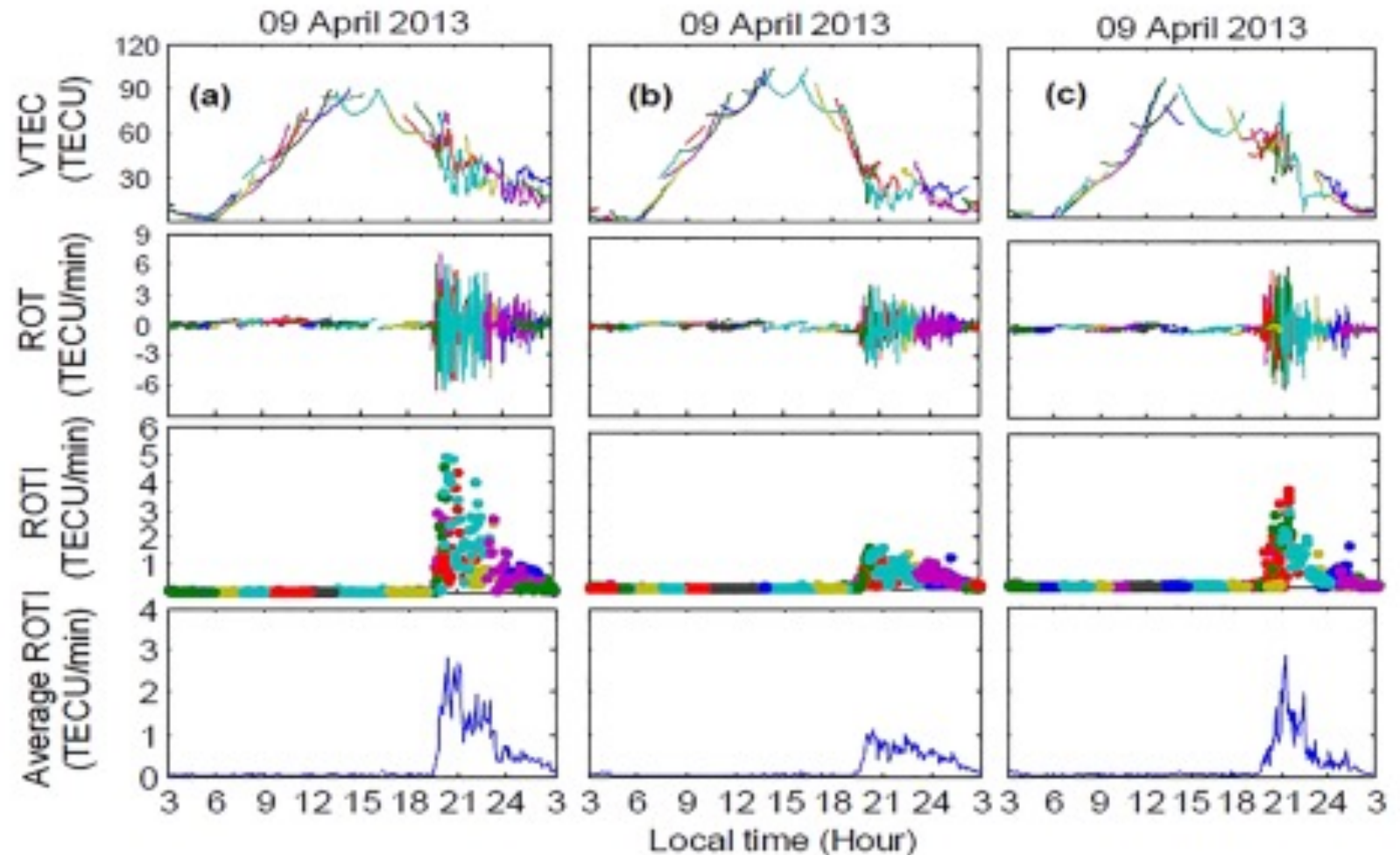


Figure 2. Typical example of ionospheric irregularities on 9th April 2013 over the (a) northern crest, (b) trough, and (c) southern crest. (first row) VTEC, (second row) ROT, (third row) ROTI, and (fourth row) average ROTI ($ROTI_{AVE}$).

Quiet-time ionospheric irregularities over the African Equatorial Ionization Anomaly (EIA) region : Monthly variation

Amaechi et al., Radio Science, 55, e2020RS007077. <https://doi.org/10.1029/2020RS007077>

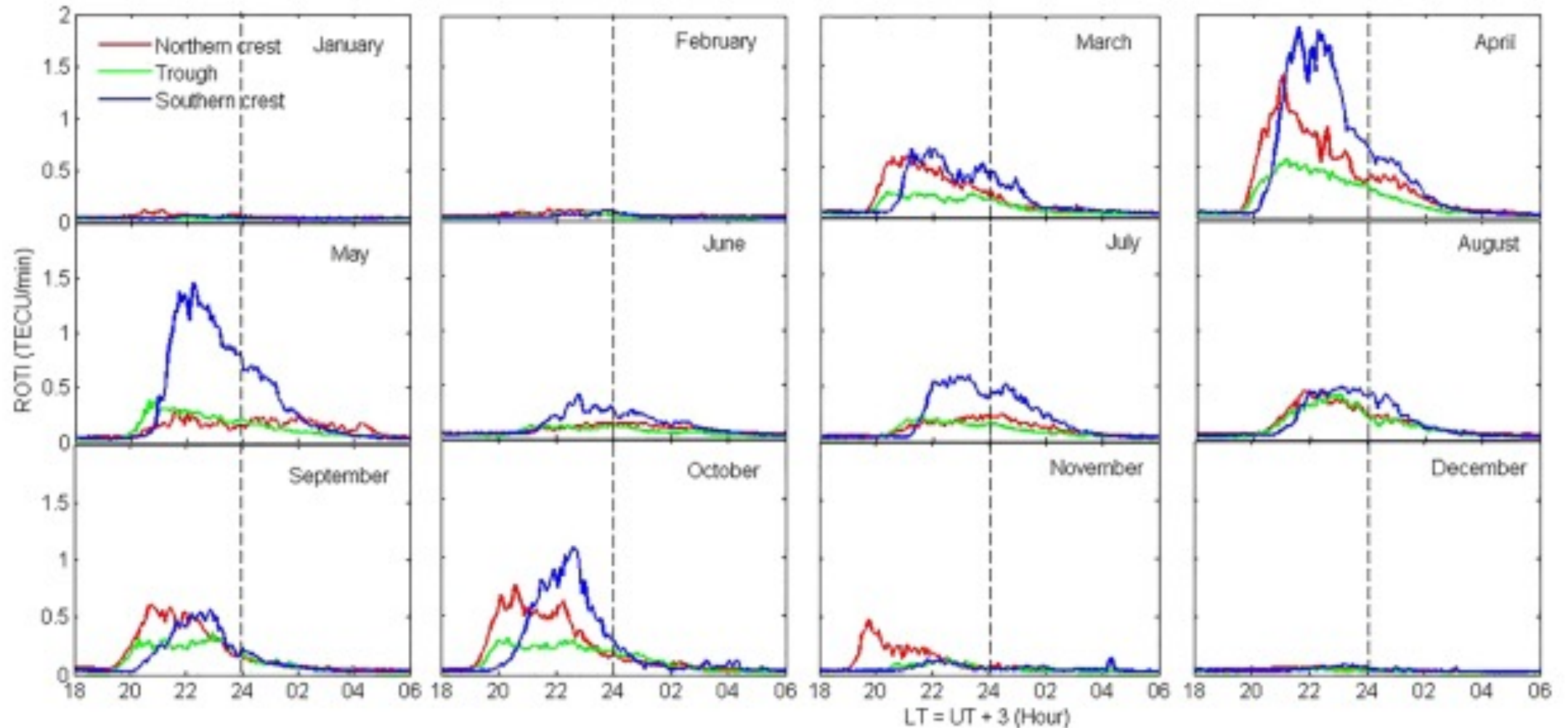
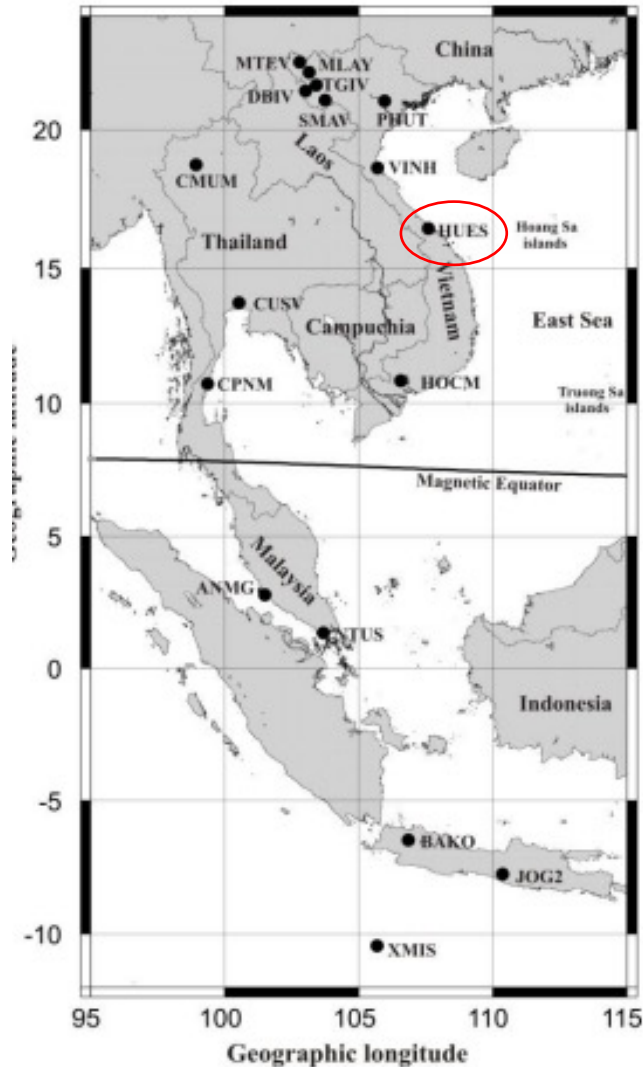


Figure 5. Monthly mean variations of quiet time irregularities over the northern crest (red line), trough (green line), and southern crest (blue line) in 2013.

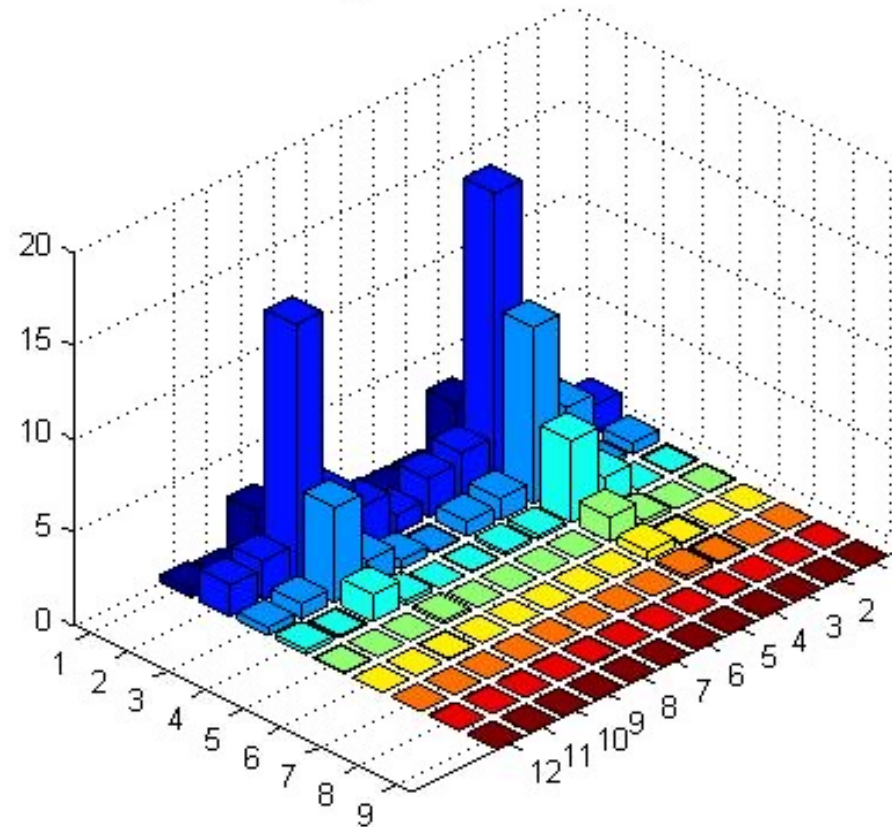
Scintillation index S4 observed at Hue during the period 2006-2008 / S4 -> fluctuations of the GPS power signal



Distribution of GPS receivers in Vietnam
And adjacent region

$$I = \frac{A^2}{2} \quad s4 = \sqrt{\frac{\langle I^2 \rangle - \langle I \rangle^2}{\langle I \rangle^2}}$$

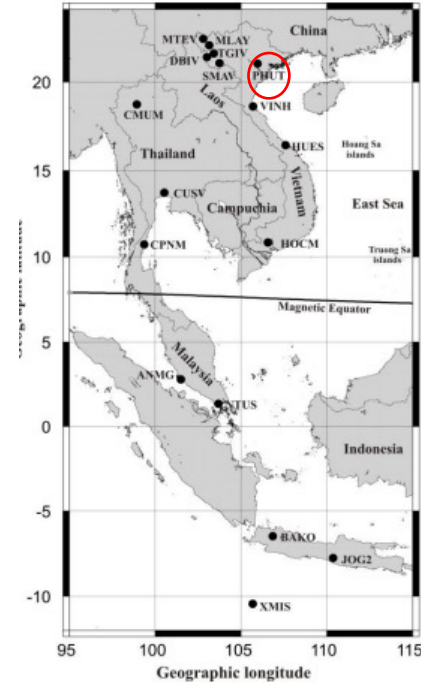
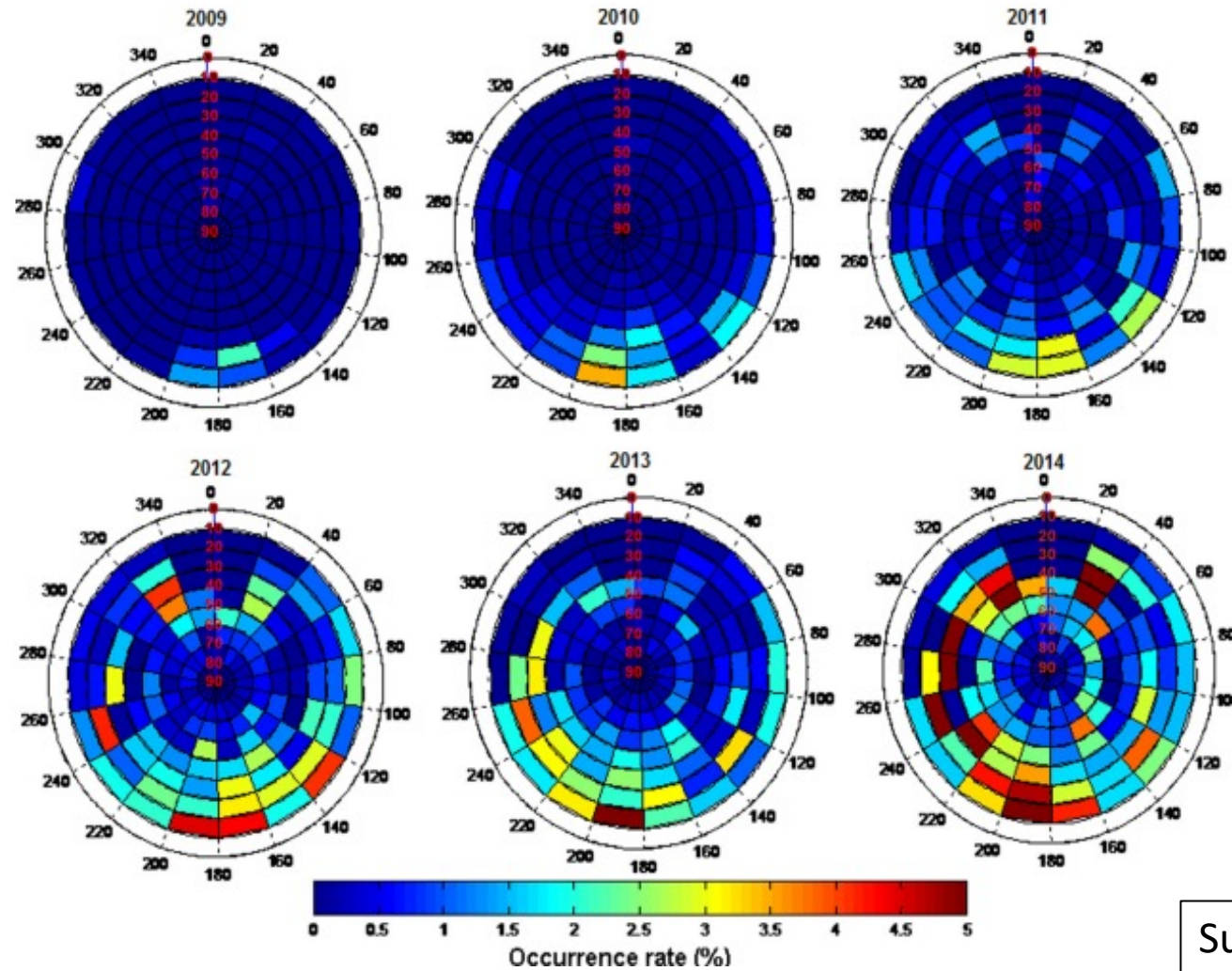
Histogram of s4 vs month - Hue



VIETNAM

The directional distribution of scintillations observed from PHUT station during 2009–2014.

VIETNAM

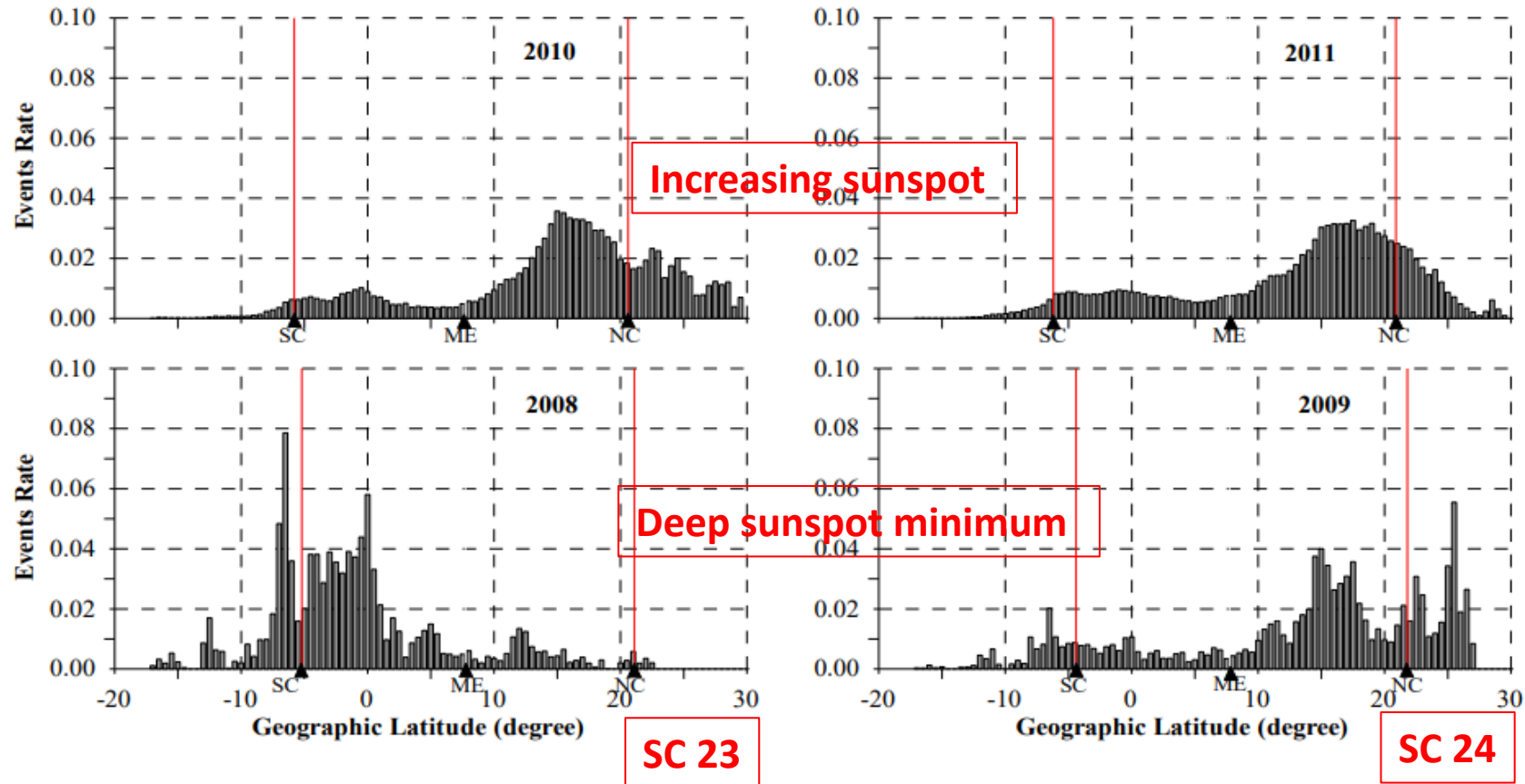


Sunspot cycle Maximum
2012,2013,2014

Tran Thi L., M. Le Huy et al.,Climatology of ionospheric scintillation over the Vietnam low-latitude region for the period 2006-2014, Advances in Space Res. <http://dx.doi.org/10.1016/j.asr.2017.05.005>.

Statistics of ionospheric irregularities ($ROTI \geq 0.5$) along geographic latitude during the period 2008-2018. ME: magnetic equatorial; SC: southern crest; NC: northern crest

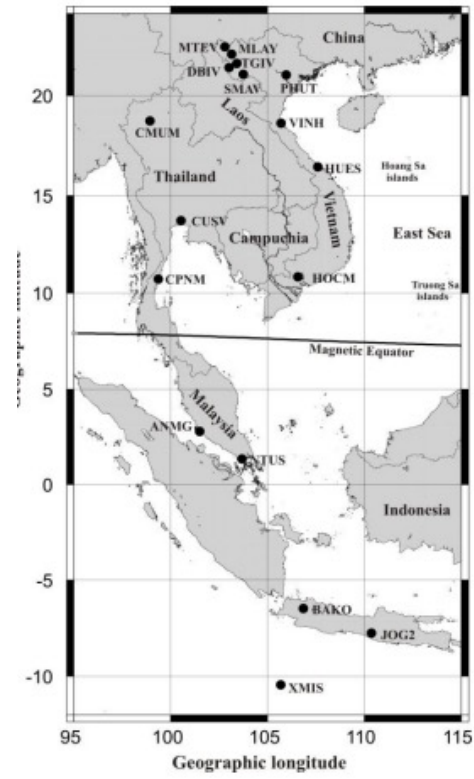
ASIAN SECTOR



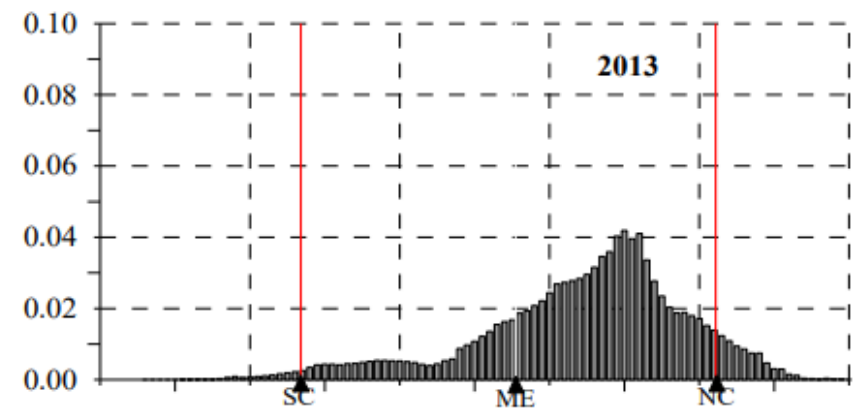
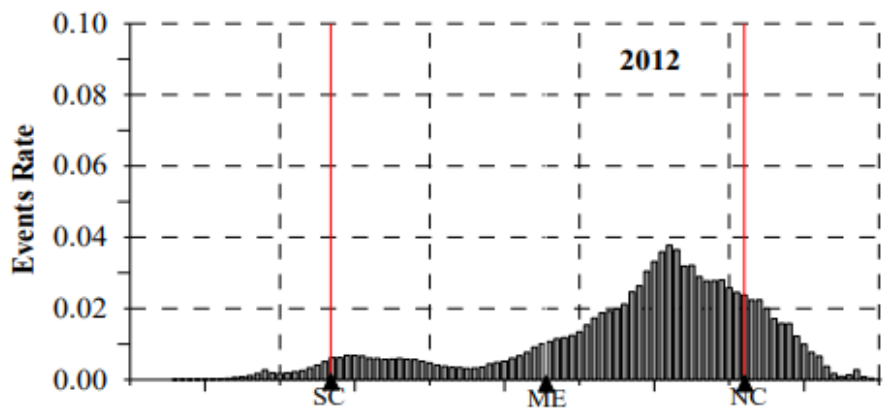
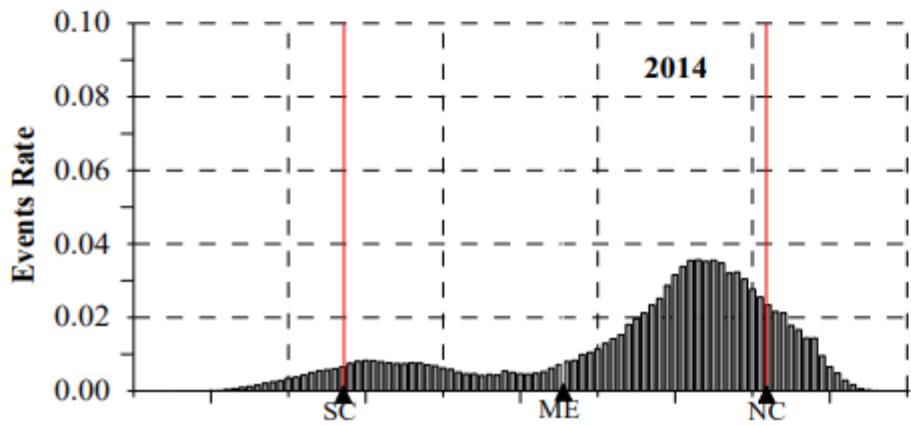
Dung Nguyen Thanh, Minh Le Huy, Christine Amory-Mazaudier, Rolland Fleury, Susumu Saito, Thang Nguyen Chien, Hong Pham Thi Thu, Thanh Le Truong, Mai Nguyen Thi, Characterization of ionospheric irregularities over Vietnam and adjacent region for the 2008-2018 period, Vietnam Journal of Earth Sciences, 1-20, <https://doi.org/10.15625/2615-9783/16502>

Statistics of ionospheric irregularities ($ROTI \geq 0.5$) along geographic latitude during the period 2008-2018.

Phase maximum of sunspot cycle 24



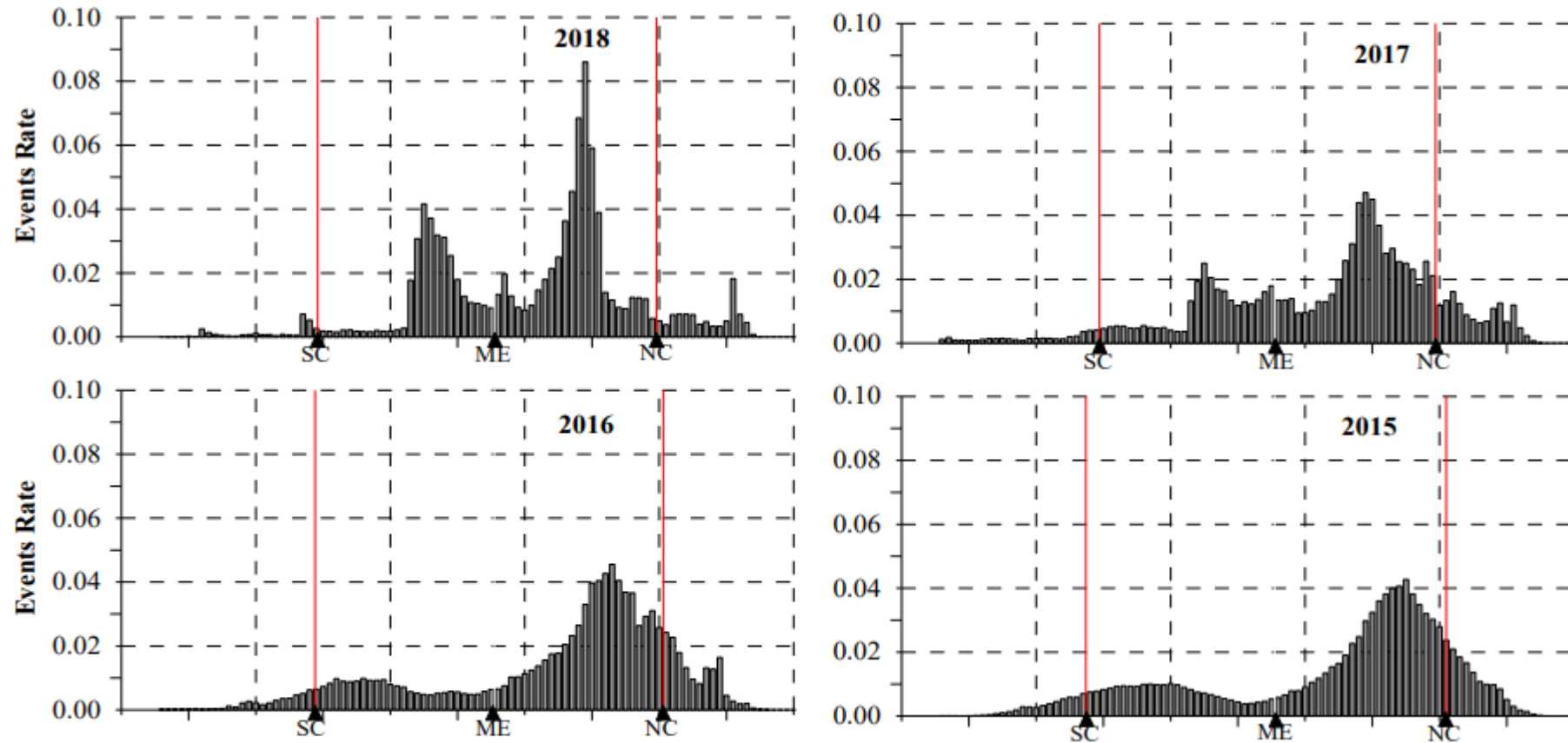
ASIAN SECTOR



Statistics of ionospheric irregularities ($\text{ROTI} \geq 0.5$) along geographic latitude during the period 2008-2018. ME: magnetic equatorial; SC: southern crest; NC: northern crest

ASIAN SECTOR

Decreasing phase of sunspot cycle 24



Outline

- Introduction
- Characteristics of the low latitudes

Equatorial Fountain, Pre Reversal Enhancement, Equatorial electrojet

- Plasma irregularities

ROTI-S4

- **Variations of ionospheric parameters due to solar electromagnetic emissions**

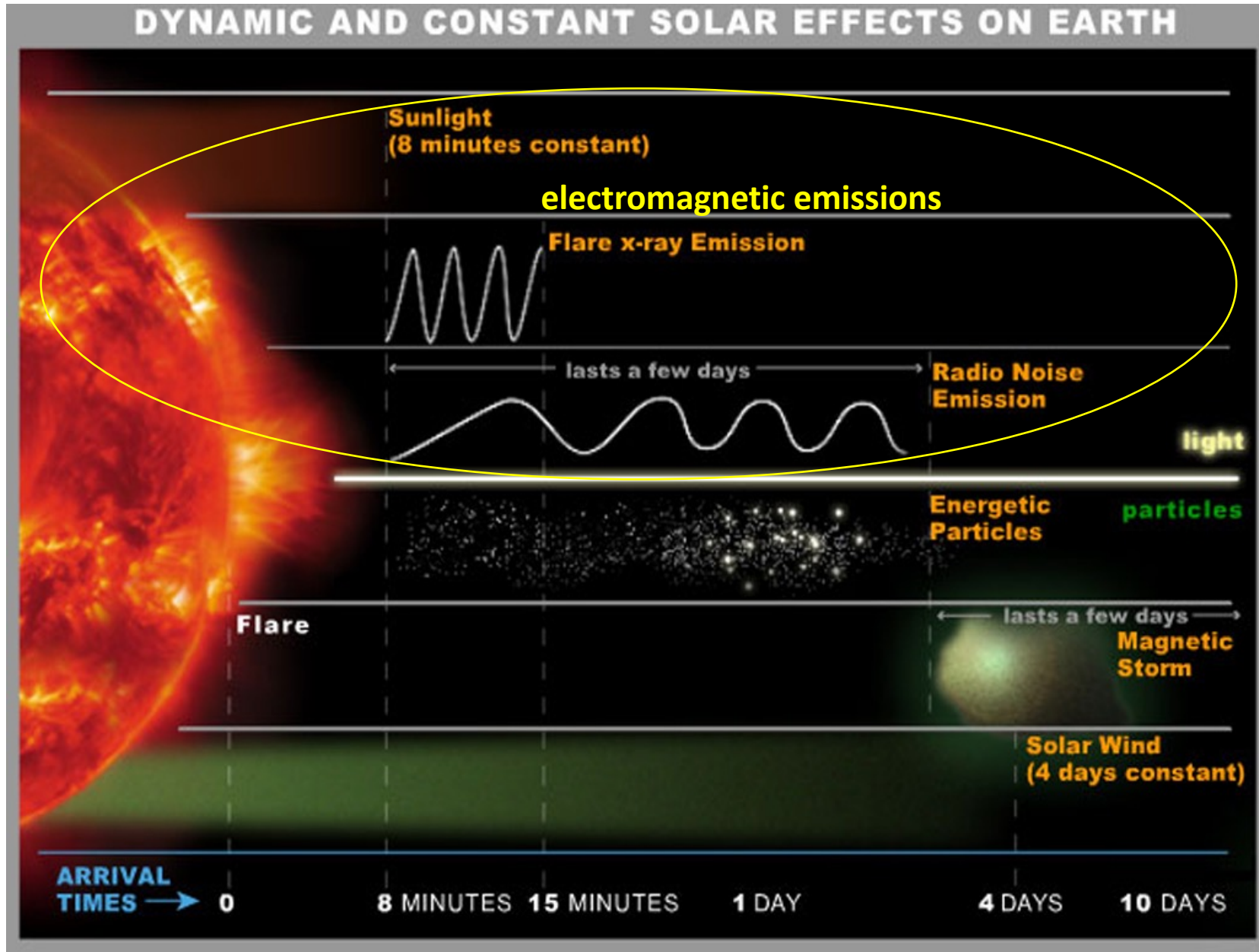
Total electron content TEC, Earth's magnetic field variations

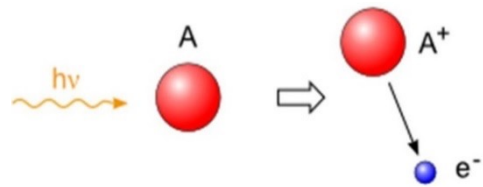
- Electrodynamical coupling between high and low latitudes

TEC, ROTI, Earth's magnetic field variations

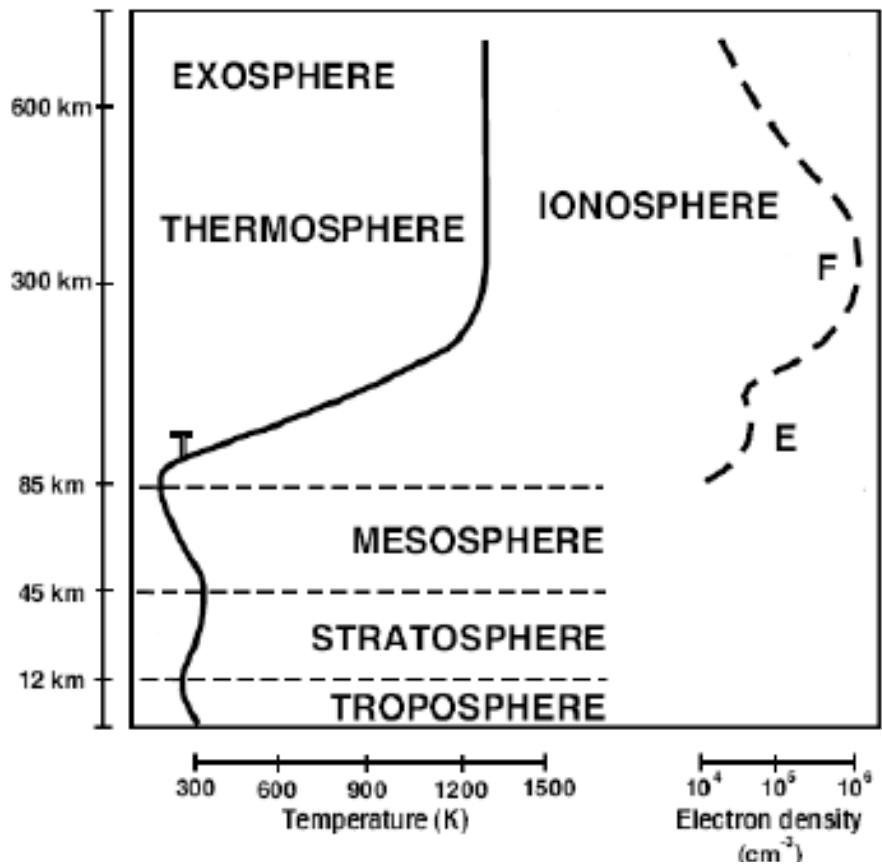
- Conclusion

SOLAR DYNAMO/ TOROIDAL COMPONENT : REGULAR RADIATIONS





The ionosphere is created by ionization of the atmosphere by UV, EUV and X radiations in the altitude range from 50 km up to ~800 km



Ionosphere is a ionized part of the atmosphere 1 atom among 1 000 000

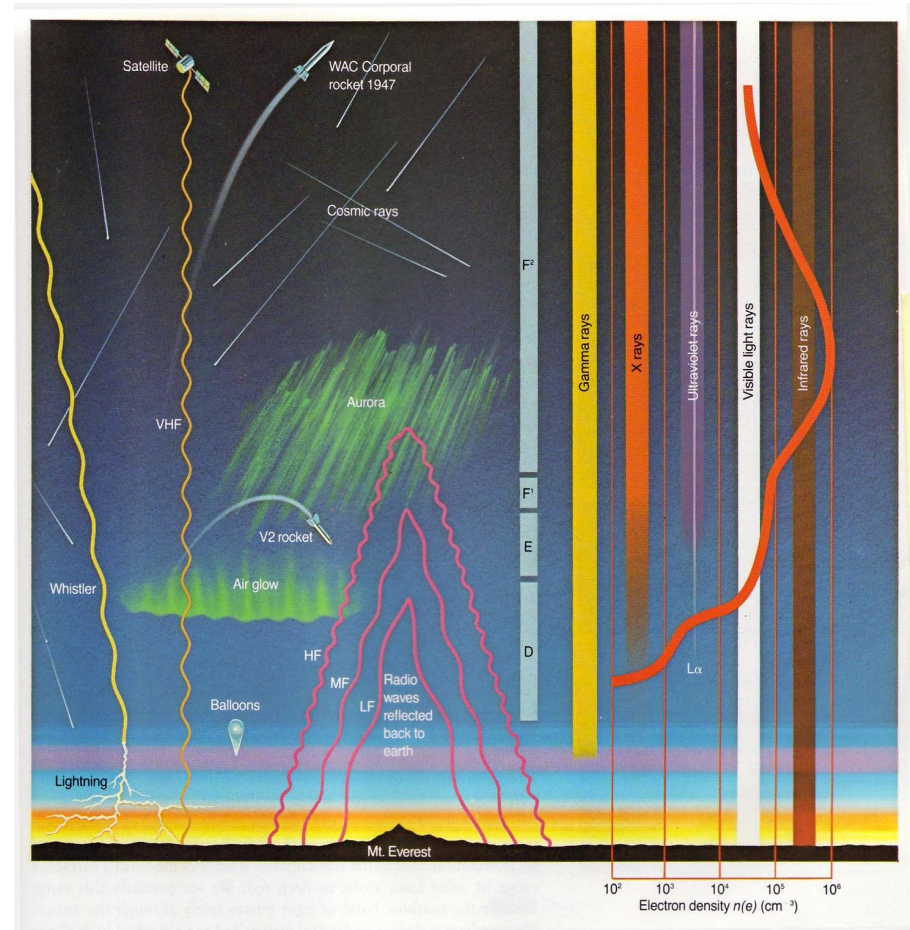
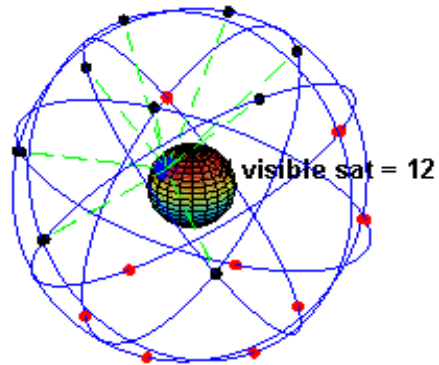
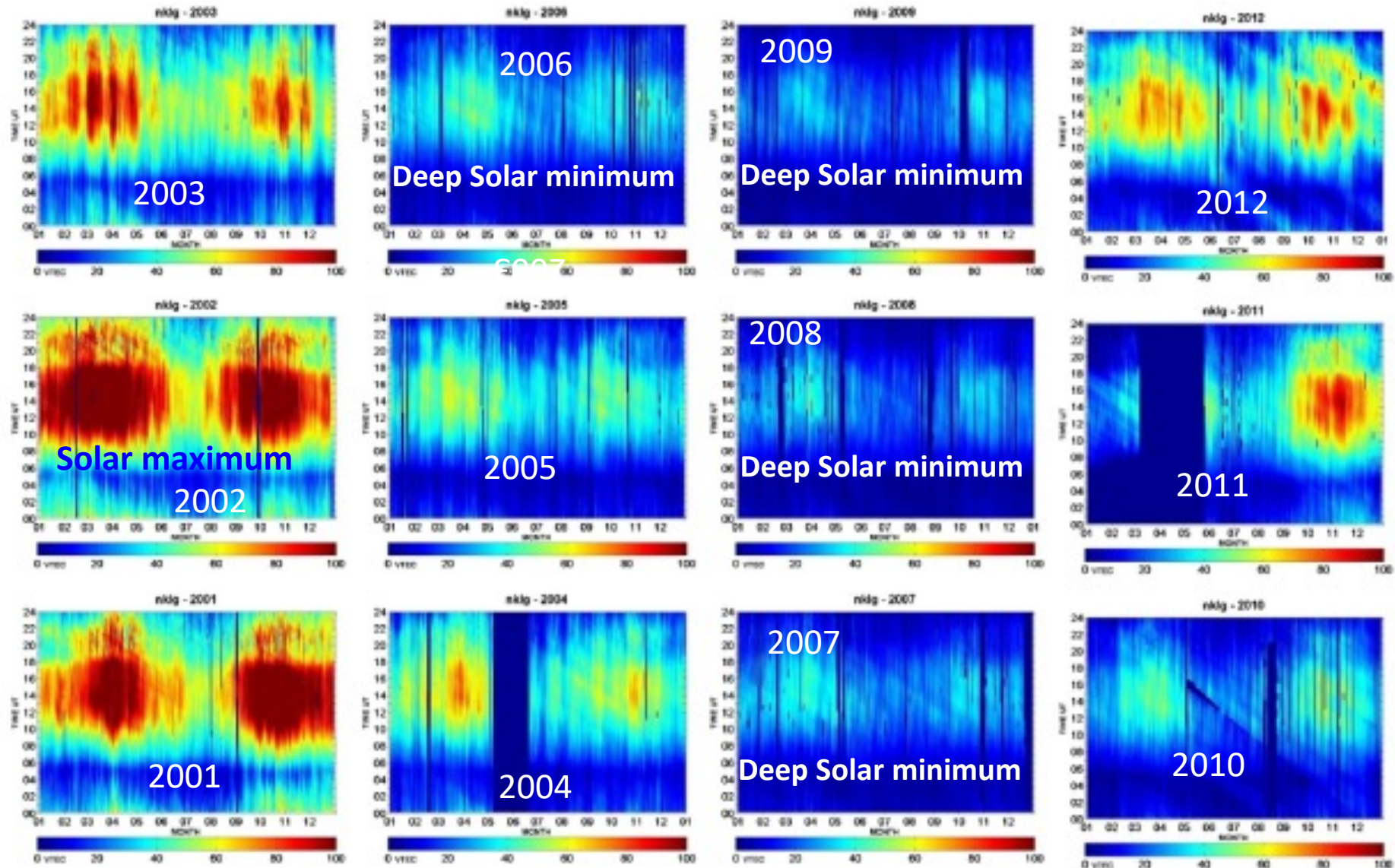


Figure from Friedman, 1987

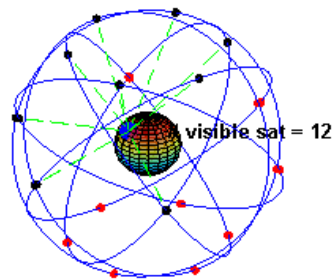
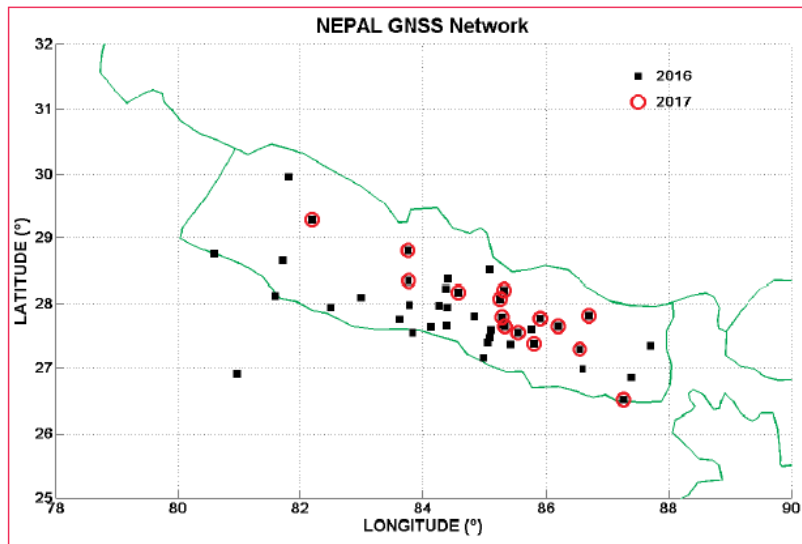
Sunspot seasonal and diurnal variation of VTEC at Libreville/Gabon



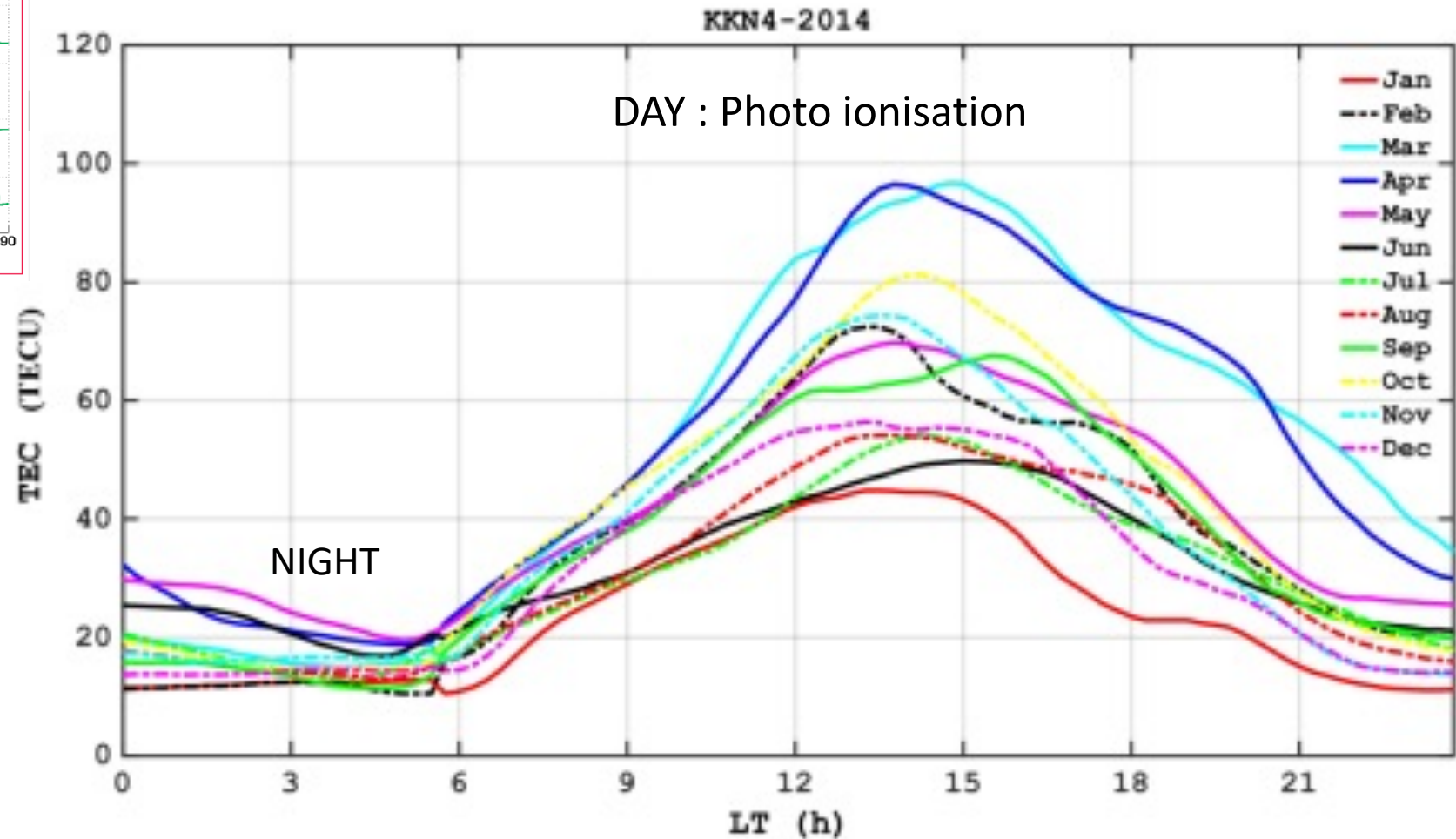
0.3539°N,
9.6721°E
Southern crest of EIA



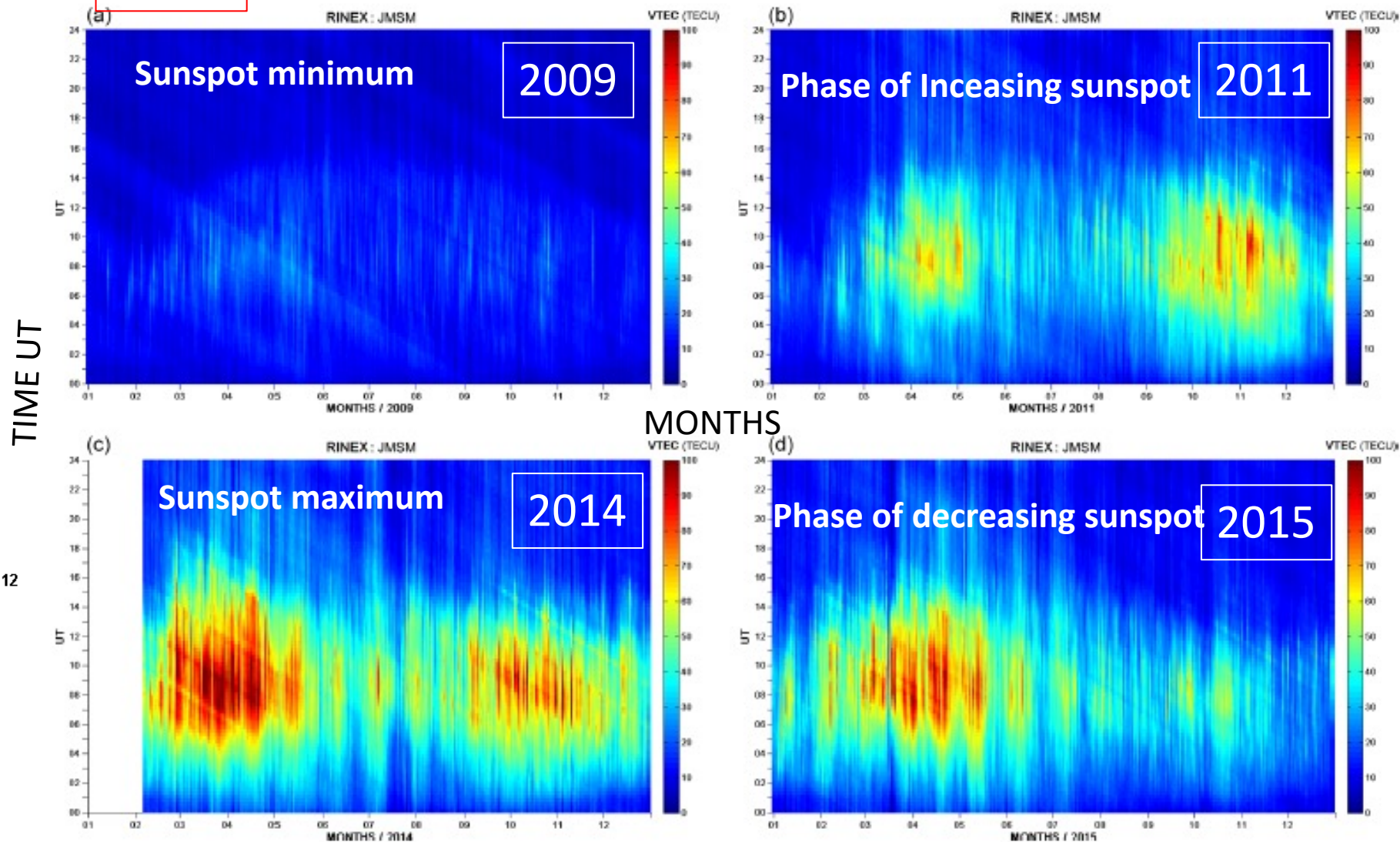
Two dimensional (2D) diurnal variation of hourly vTEC at NKLG from 2002 to 2012. Shimeis et al., Advances in Space Research 54 (2014) 2159–2171.



Monthly variation in vertical TEC in LT for each month of 2014 at KKN4 station.



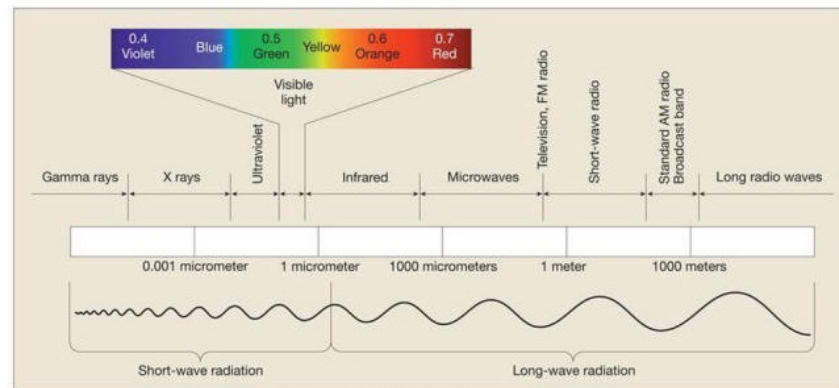
Pandit, D. B. Ghimire, C. Amory-Mazaudier, R. Fleury, N. P. Chapagain, B. Adhikari, Climatology of ionosphere over Nepal based on GPS TEC data from 2008 to 2018, *Ann. Geophys.*, 39, 743–758, 2021 <https://doi.org/10.5194/angeo-39-743-2021>



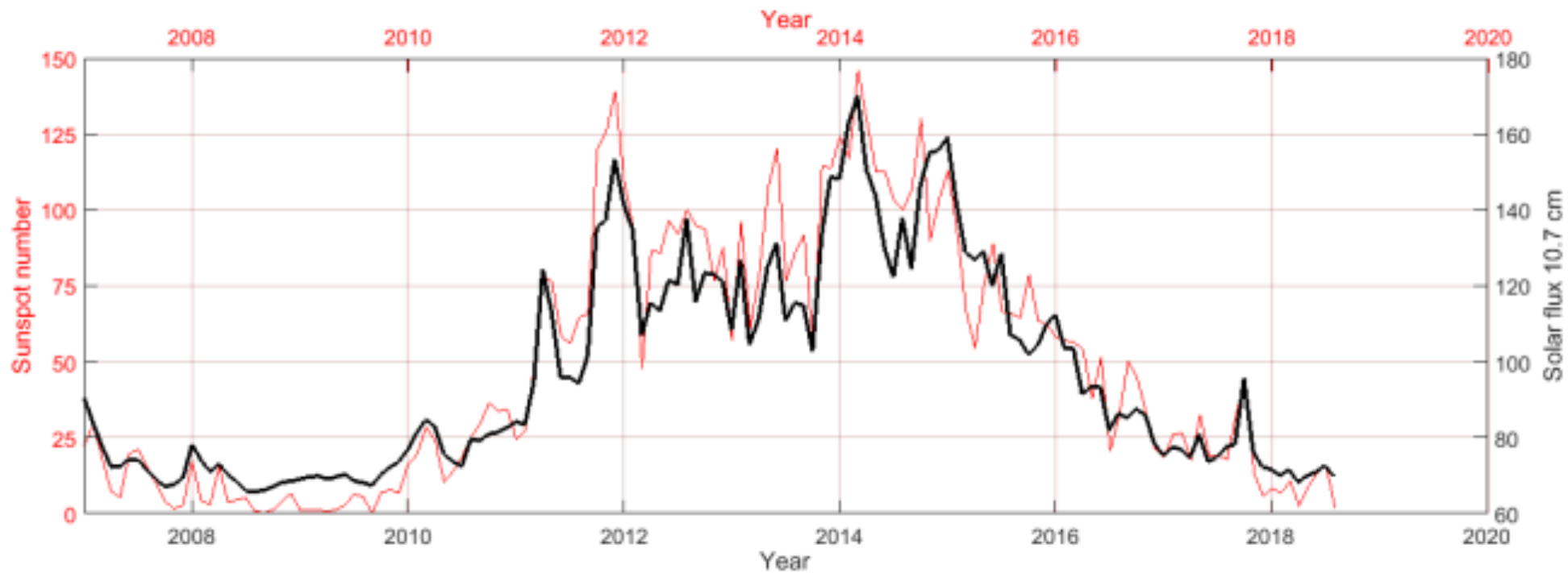
(a–d) A two-dimensional (2D) variation in vertical TEC according to UT at the JMSM station for one of the years of the minimum (2009), ascending (2011), maximum (2014) and descending (2015) phases of solar cycle 24.

Solar electromagnetic emissions/ Sunspot cycle

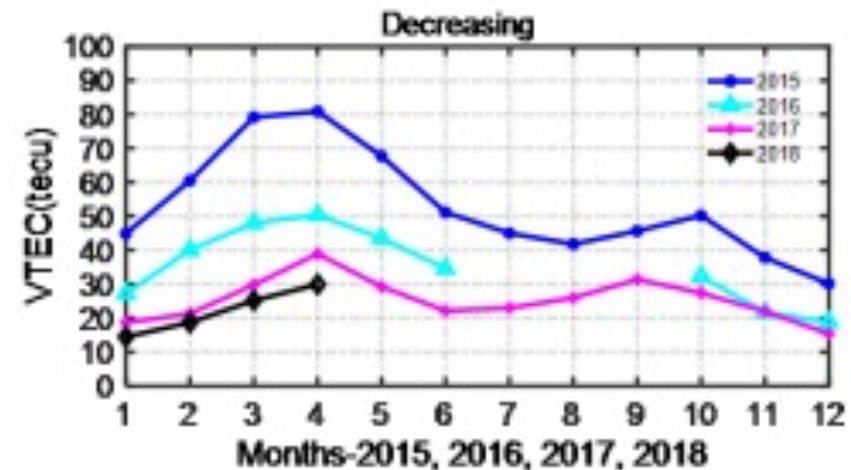
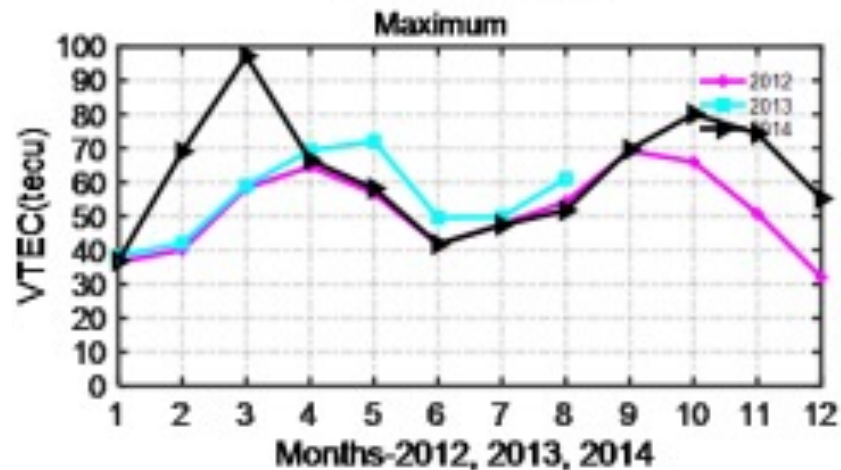
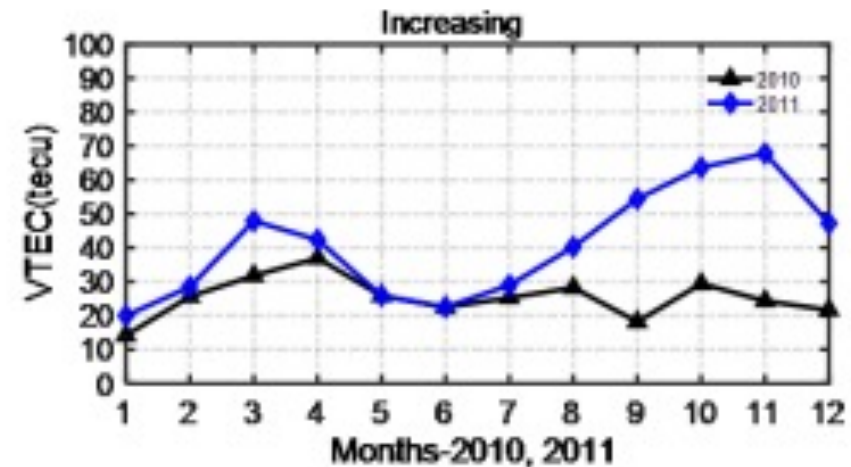
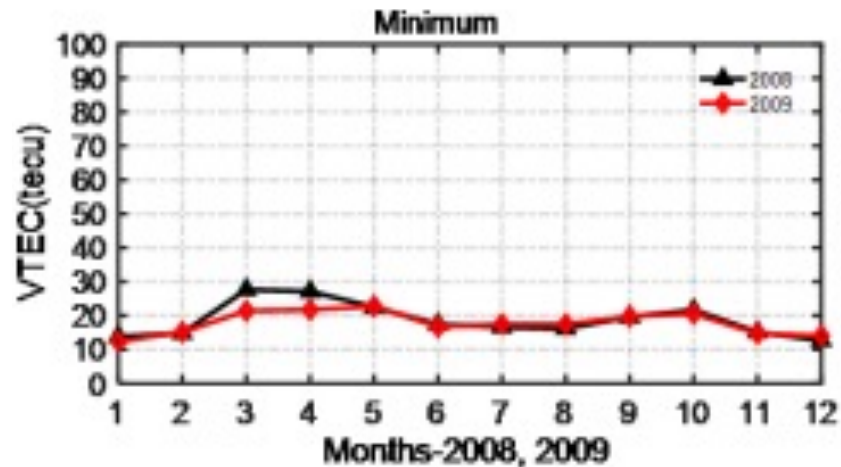
PHYSICS



Copyright © 2007 Pearson Prentice Hall, Inc.



PHASES OF SUNSPOT CYCLE

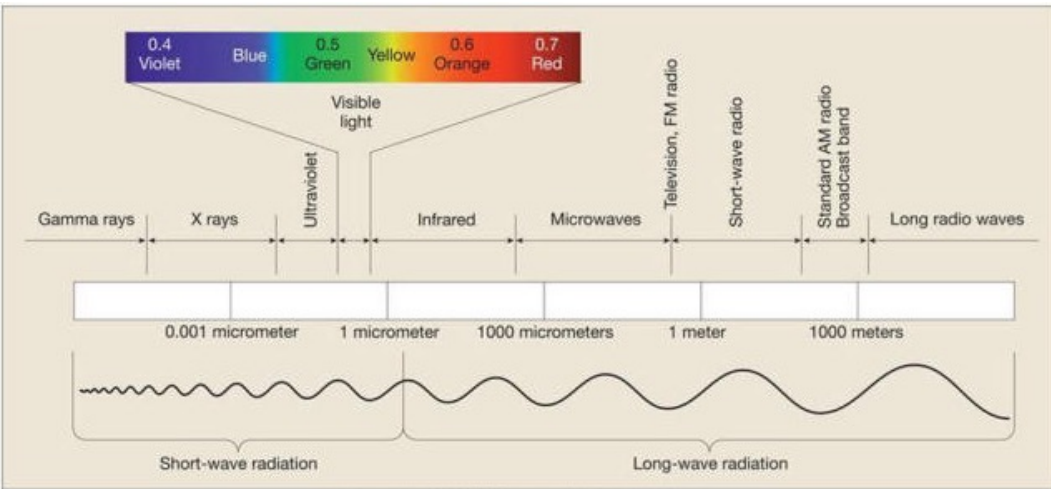


VTEC variability in GRHI station during minimum, increasing, maximum and decreasing phases of solar cycle 24

Ionospheric Dynamo

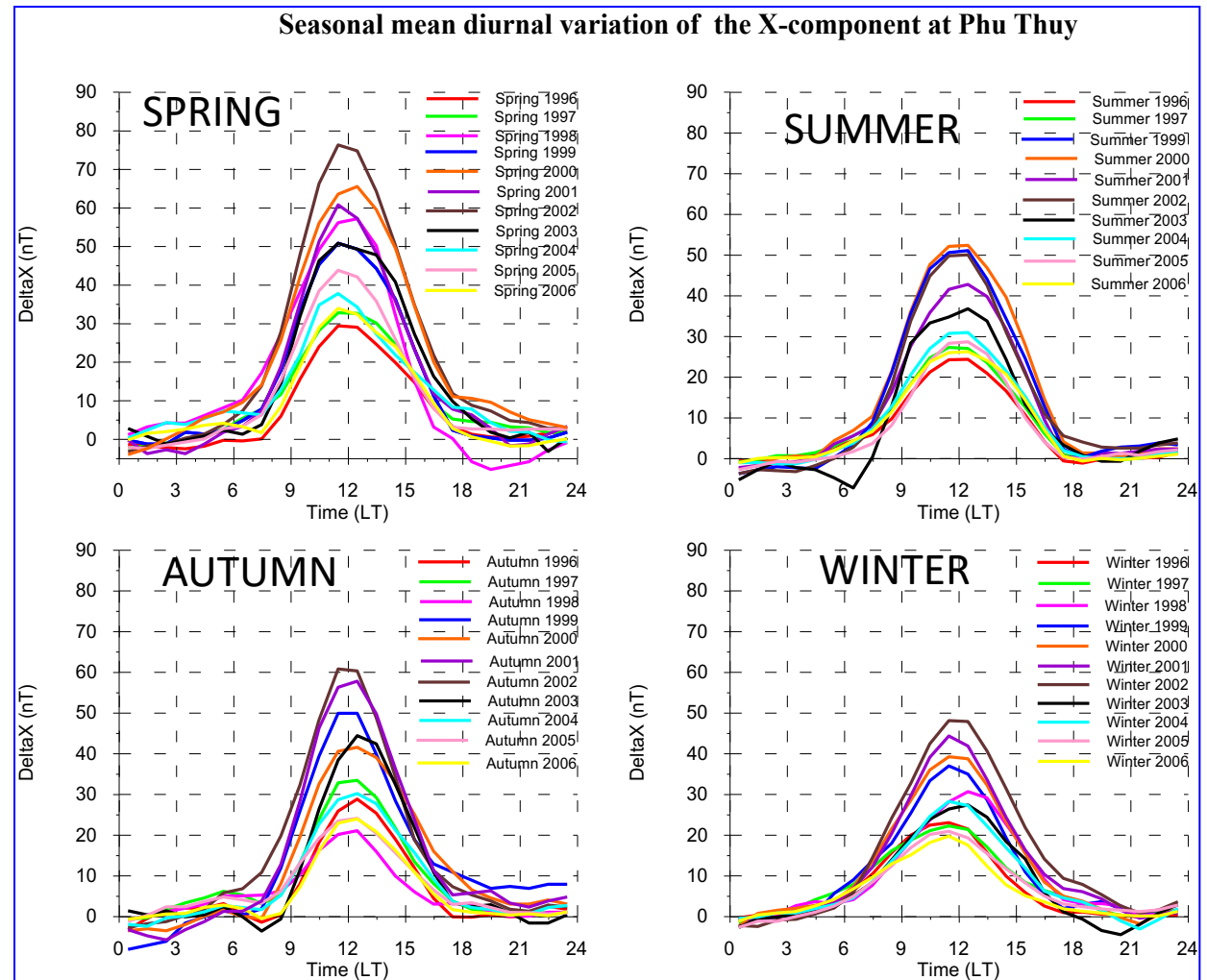
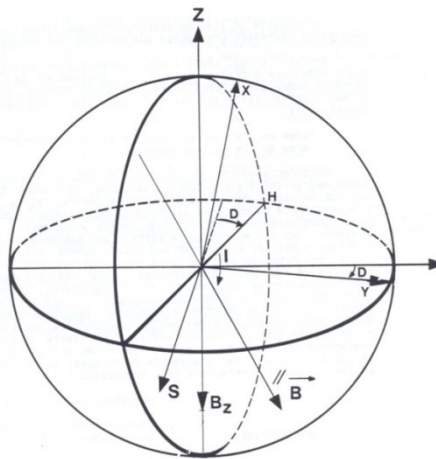
Toroïdal component of the solar magnetic field [Sunspots]

=> Solar Radiations EUV, UV => Ionosphere=> ionospheric electric current => Regular variation of the Earth's on magnetic quiet days (K_p or $K_m < 2+$)



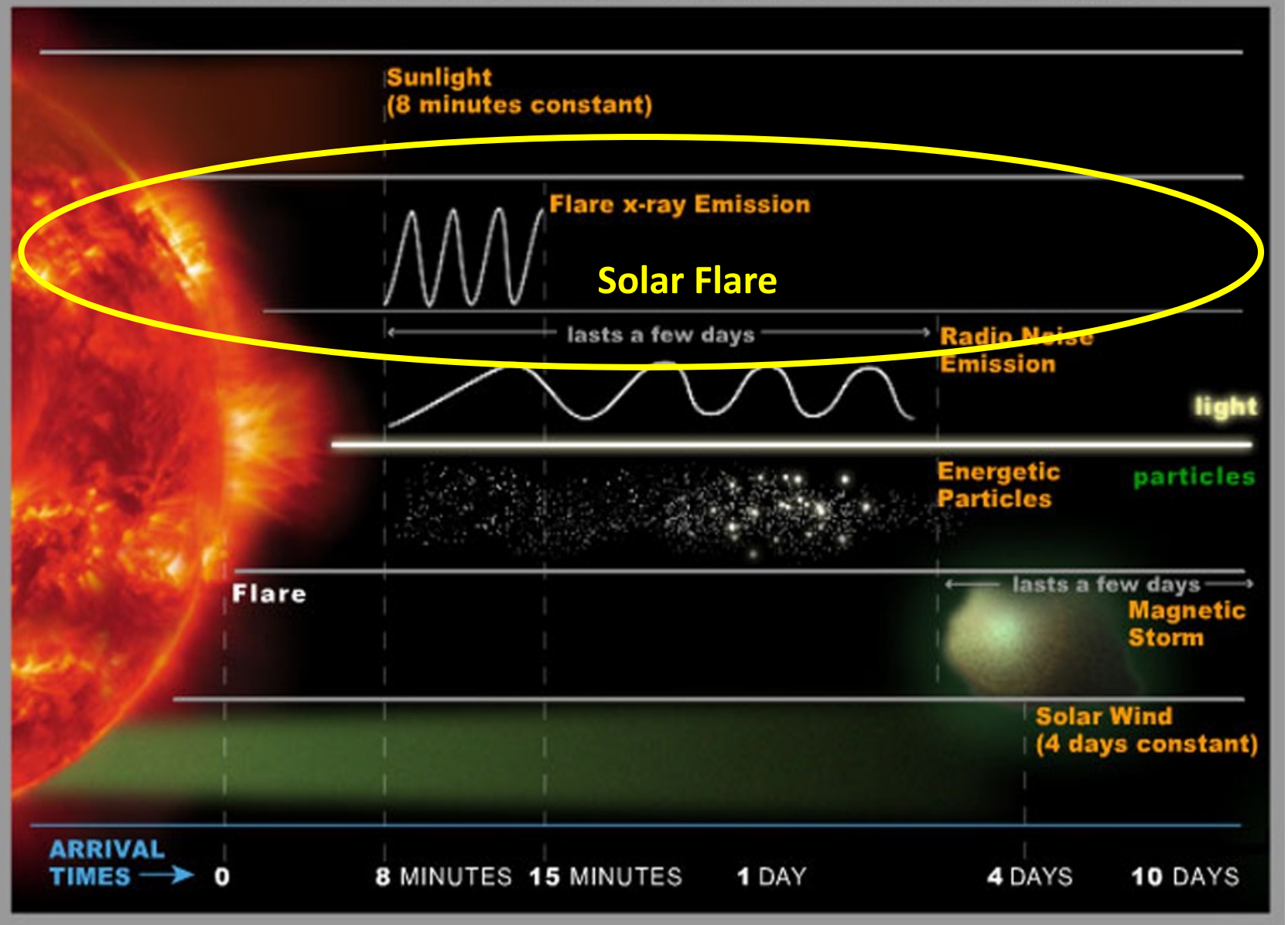
Copyright © 2007 Pearson Prentice Hall, Inc.

Images du satellite SOHO
NASA - ESA



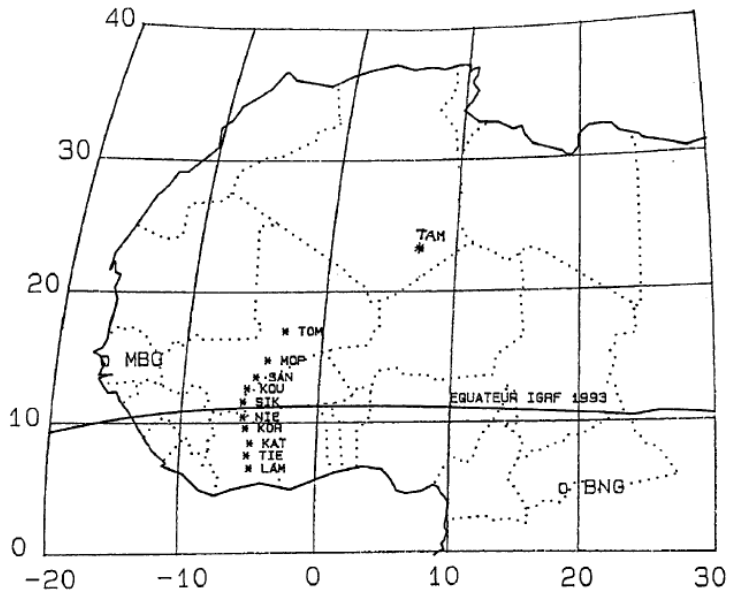
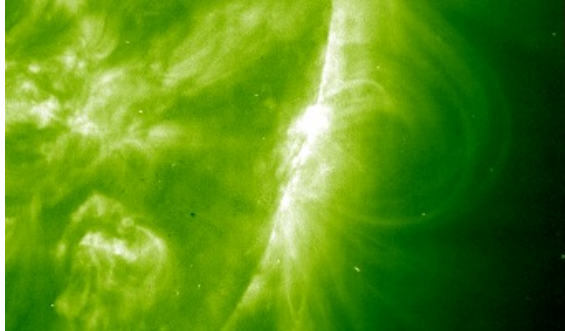
X component of the Earth's magnetic Field at Phu Thuy/ Vietnam

DYNAMIC AND CONSTANT SOLAR EFFECTS ON EARTH



Geo-electric field variations due to the solar flare on 04 April, 1993

Solar Flare
extra electromagnetic emissions



Magneto telluric station
Côte d'Ivoire

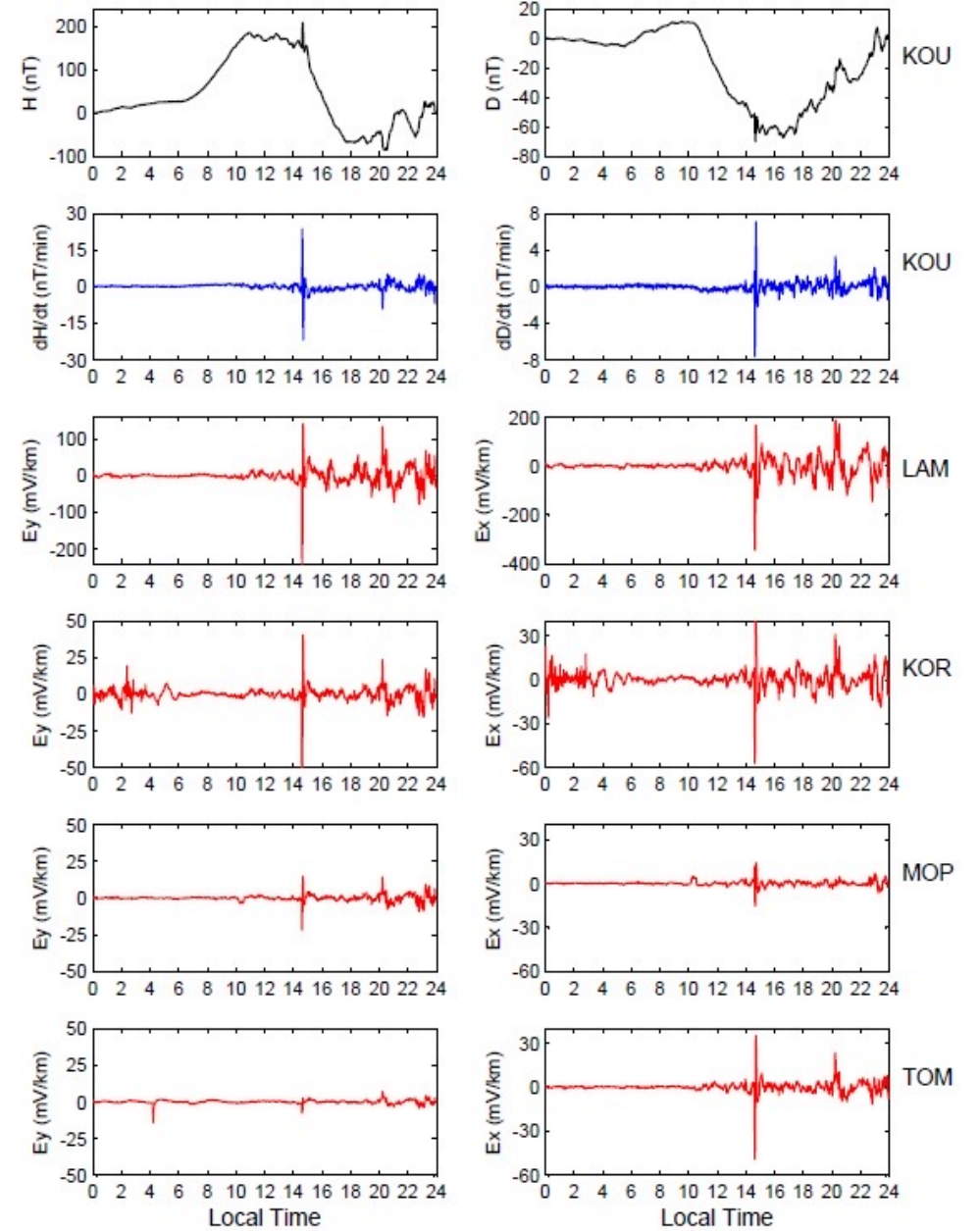
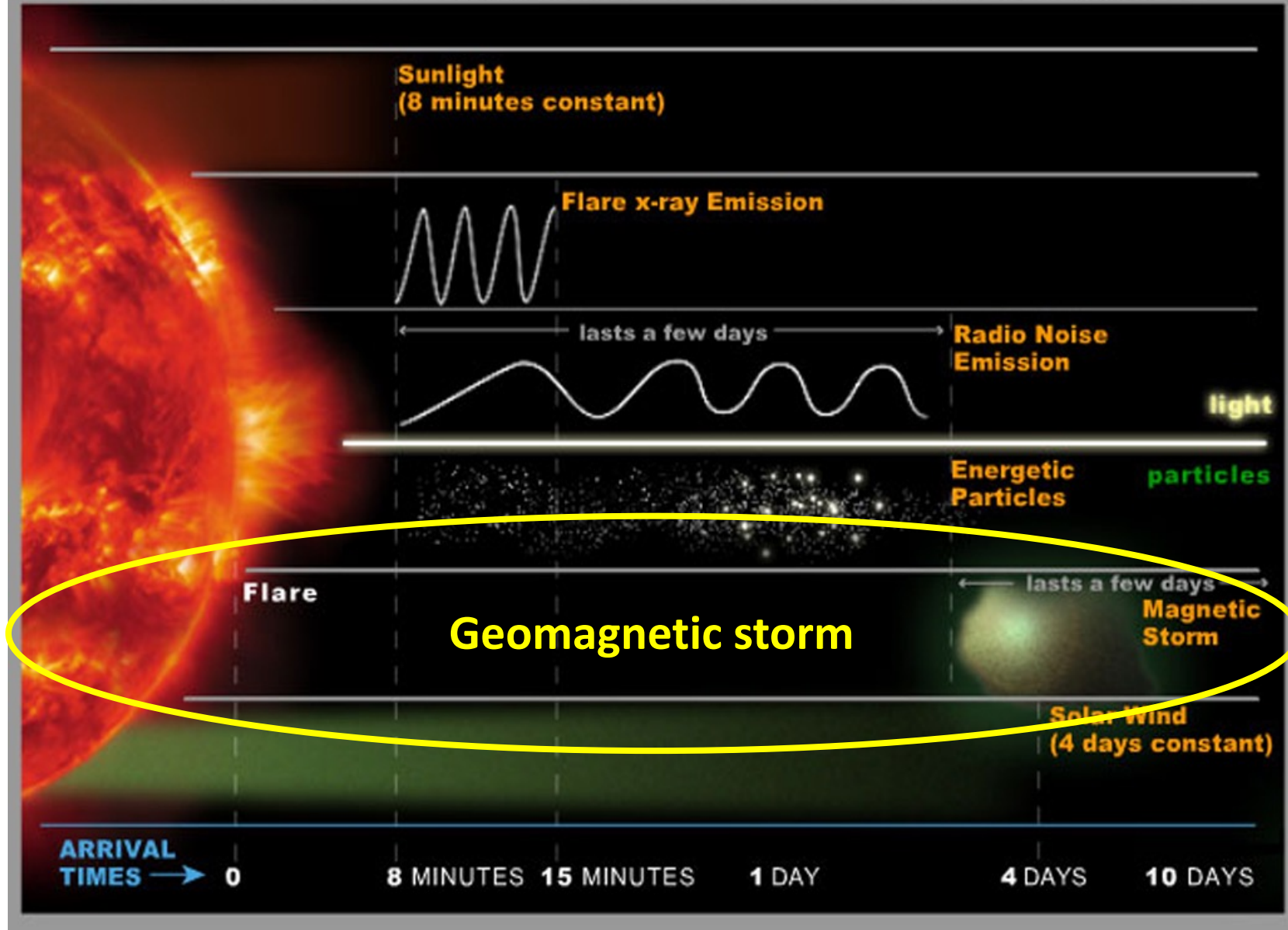


Fig. 1. Experimentation sites of the African sector during the IEEY project.

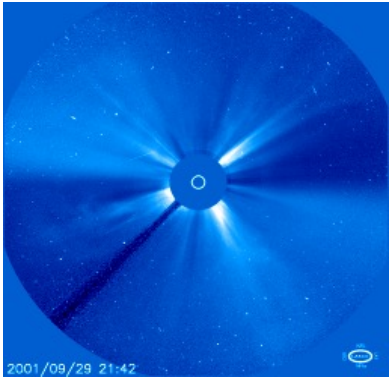
Outline

- Introduction
- Characteristics of the low latitudes
Equatorial Fountain, Pre Reversal Enhancement, Equatorial electrojet
- Plasma irregularities
ROTI-S4
- Variations of ionospheric parameters due to solar electromagnetic emissions
Total electron content TEC, Earth's magnetic field variations
- **Electrodynamic coupling between high and low latitudes**
TEC, ROTI, Earth's magnetic field variations
- Conclusion

DYNAMIC AND CONSTANT SOLAR EFFECTS ON EARTH



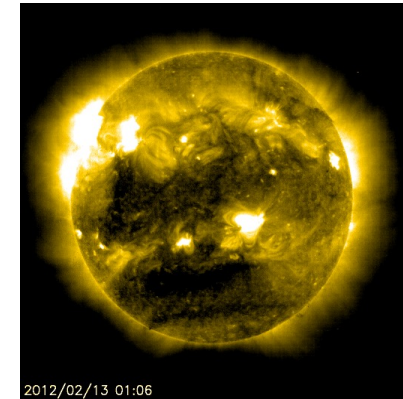
CME: Coronal Mass Ejection
Magnetic cloud



SUN-EARTH CONNECTIONS

Solar wind
from the Sun to the Earth

Coronal hole
HSSW - CIR



Coupling between high and low latitudes

1. Transmission of an **electric field PPEF**

*Magnetic disturbance **DP₂** (large scale disturbed ionospheric electric current)*

2.a Thermal expansion of the atmosphere

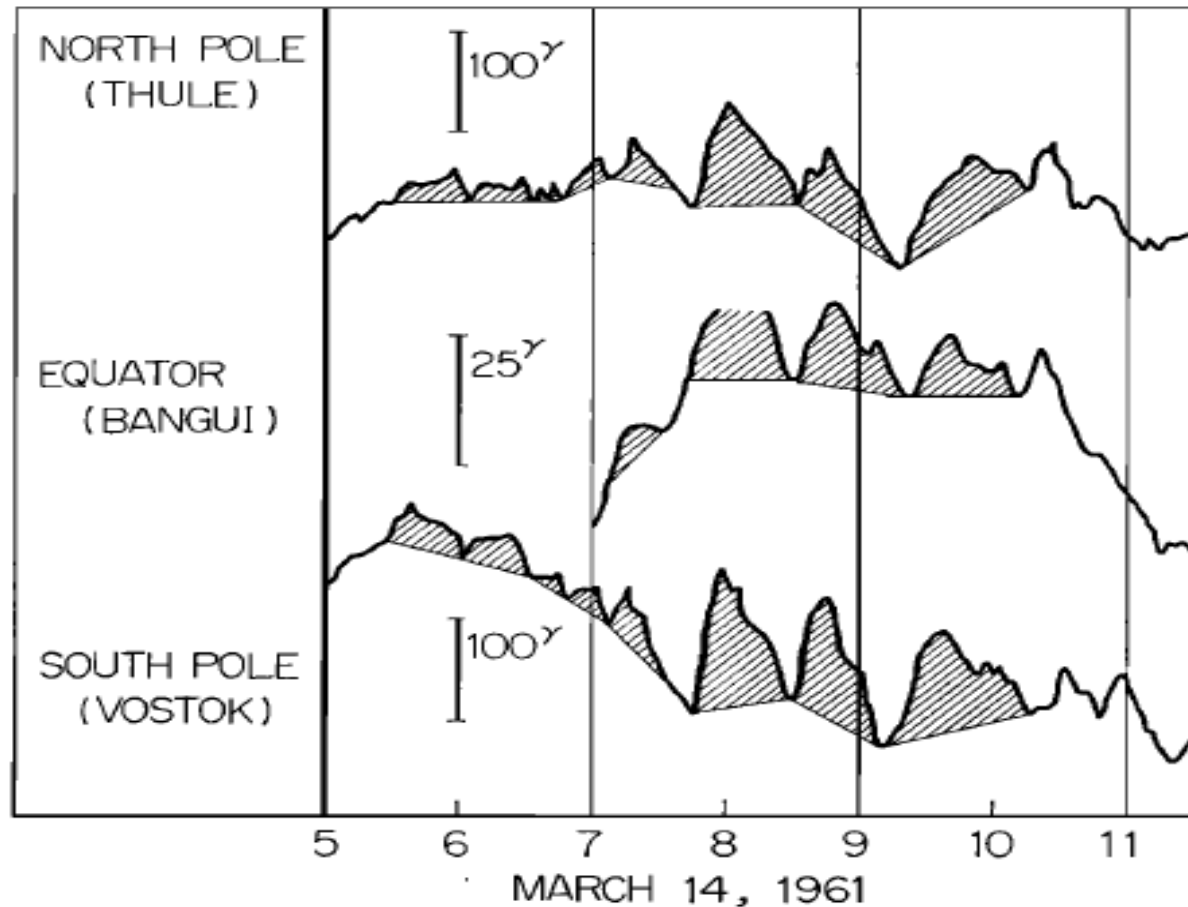
Changes in pressure, temperature, motions, composition

2.b Transmission of a disturbance **electric field dynamo DDEF** by the disturbed atmospheric **motions in the dynamo layer**

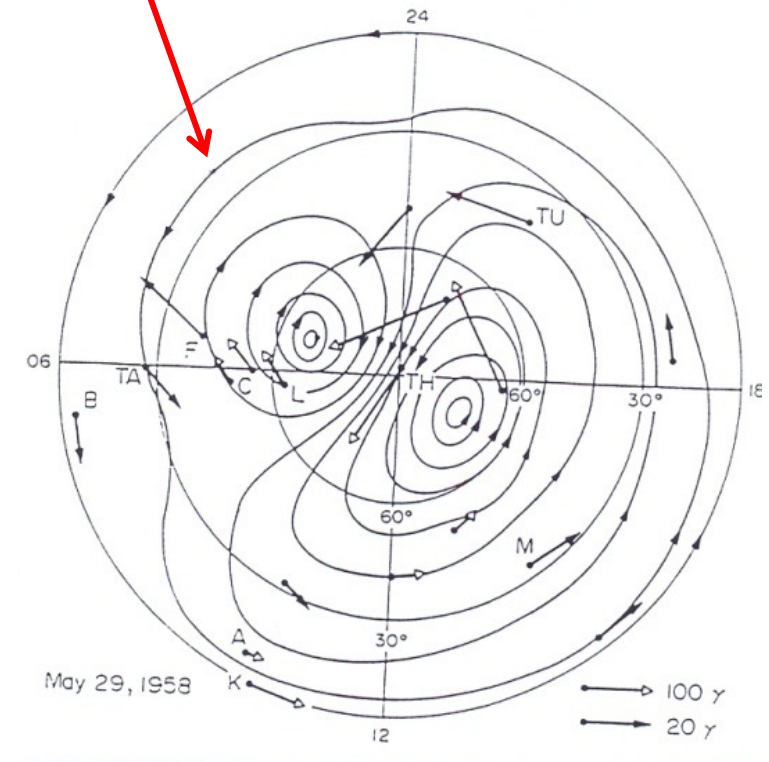
*Magnetic disturbance **Ddyn** (large scale disturbed ionospheric electric current)*

COUPLING between AURORAL and EQUATORIAL regions THE MAGNETIC EQUIVALENT CURRENT SYSTEM DP₂

DP₂, Nishida, 1968, JGR, Ce système de courant s'étend vers les basses latitudes (perturbation magnétique [Nishida et al., 1966])

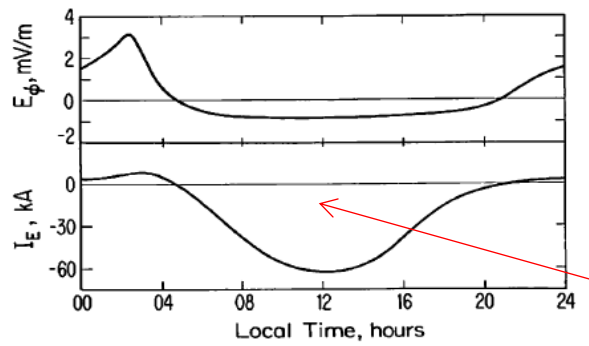
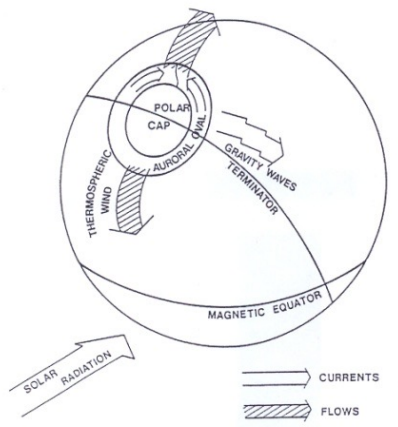
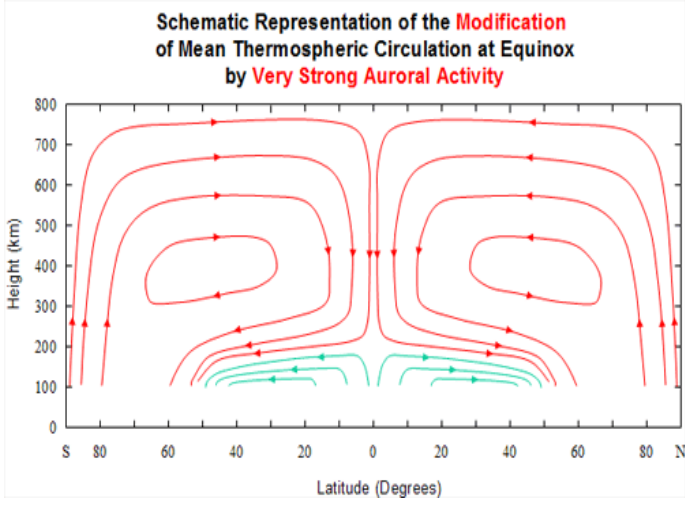
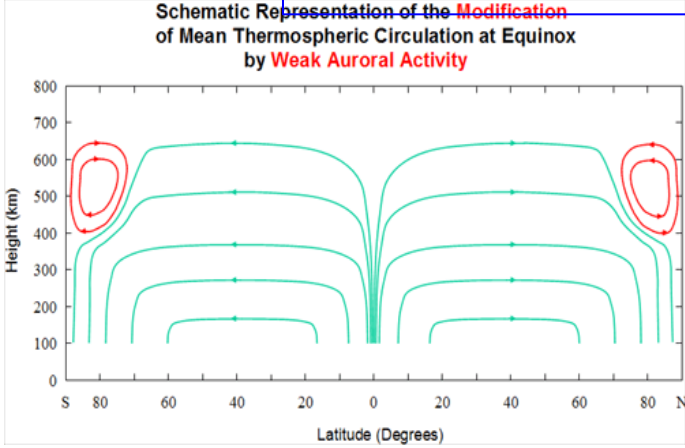


Train of $D_p 2$ fluctuations (shaded). Geomagnetic latitudes of these stations are 88.9 (Thule), 05.0 (Bangui), and -89.1 (Vostok).



Magnetic disturbance from the Pole to the Equator : D_{dyn}

The Ionospheric Disturbance Dynamo (Blanc and Richmond , JGR 1980) : **model**
 Le Huy and Amory-Mazaudier JGR 2005 : **magnetic disturbance D_{dyn}**
 This physical process related to the circulation of thermospheric winds disturbed by the storm takes several hours to reach the equator



Blanc and Richmond, 1980.

JOULE HEATING in auroral zone [AE]
 ΔV_n : disturbance of wind, circulation from pole to Equator
 Gravity waves, HADLEY convection cell etc...
 $*\Delta E_{dyn}$: disturbance of Electric field due to storm winds
 $*\Delta J$: Disturbance of ionospheric electric current
 $*\Delta B$: Disturbance of the Earth's magnetic field D_{dyn} due to a reversed electrojet

Thermal expansion of the atmosphere: Travelling Atmospheric disturbance (TAD's) => disturbed TEC [Theory Fuller Rowell et al., (1994), (1996)]

24/08/2005

SSC : 13.00 UT

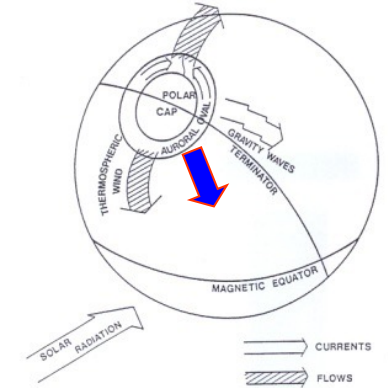
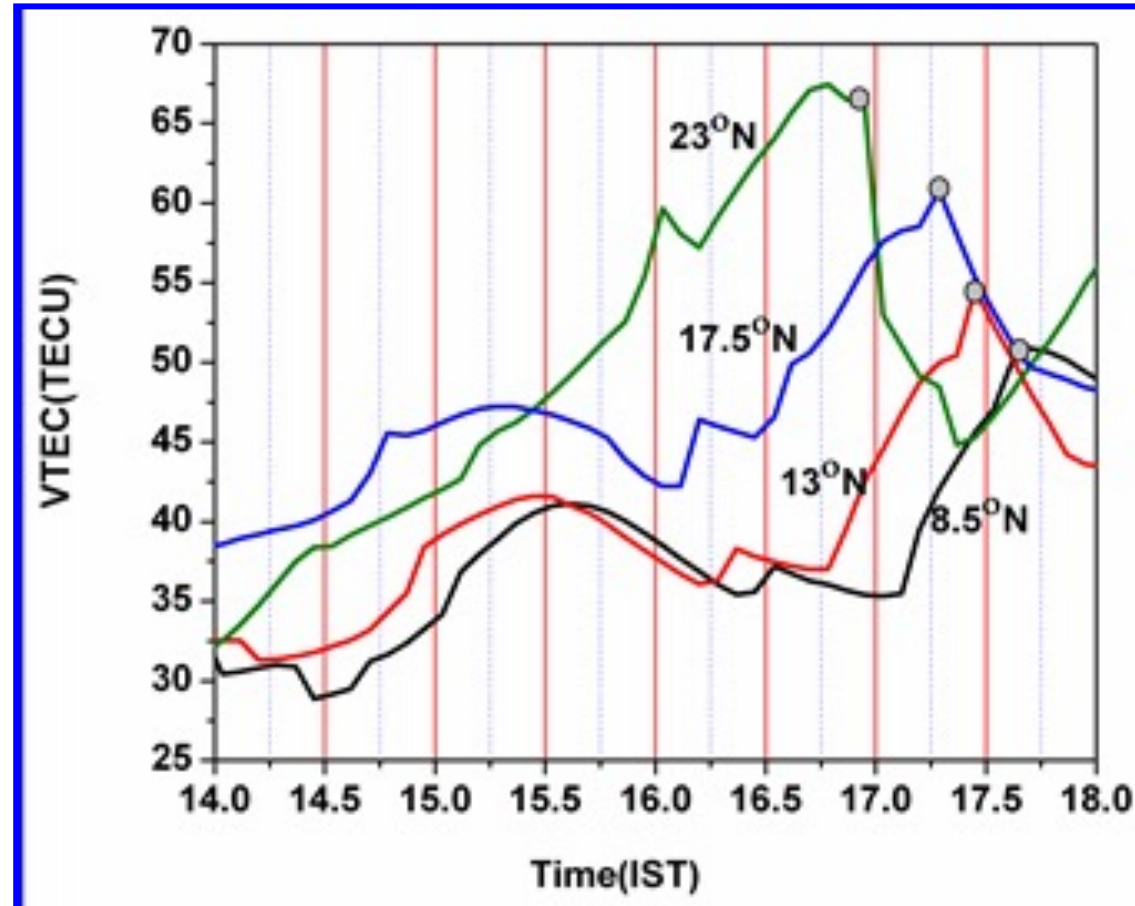
Main Phase : 16 00 UT

INDIA

77-78°E meridian

V~750m/s

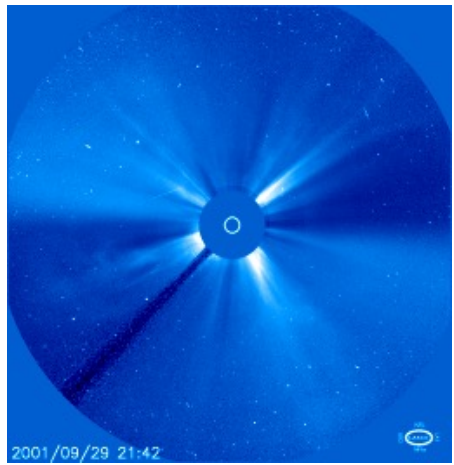
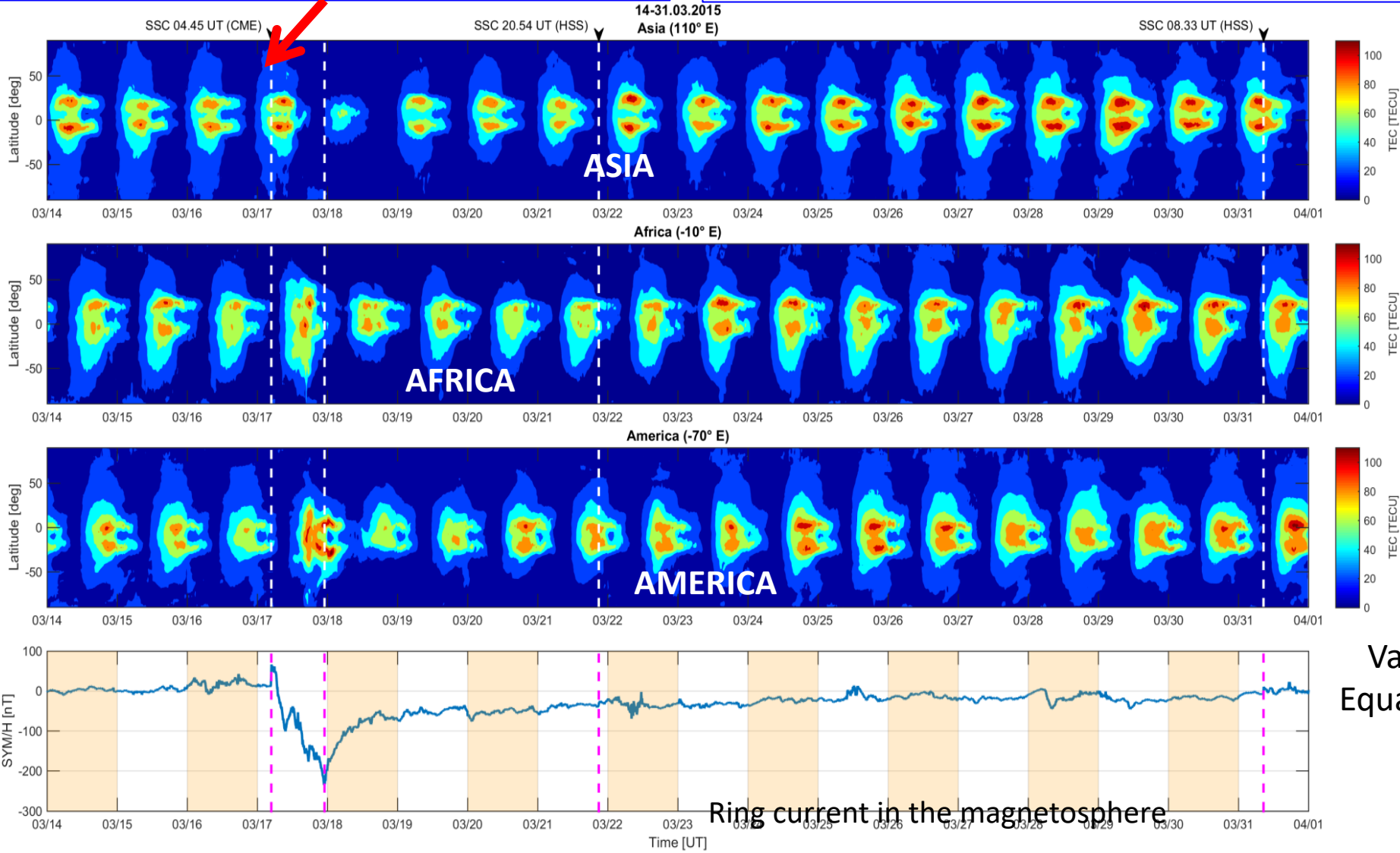
Sreeja et al.,
JGR vol 114, A12307, 2009



A time delay in the VTEC variations over the different latitudes indicates a propagation of TAD's Velocity 750m/s

Impact of a CME (solar event, SSC on March 17
 ~ 04.45UT)

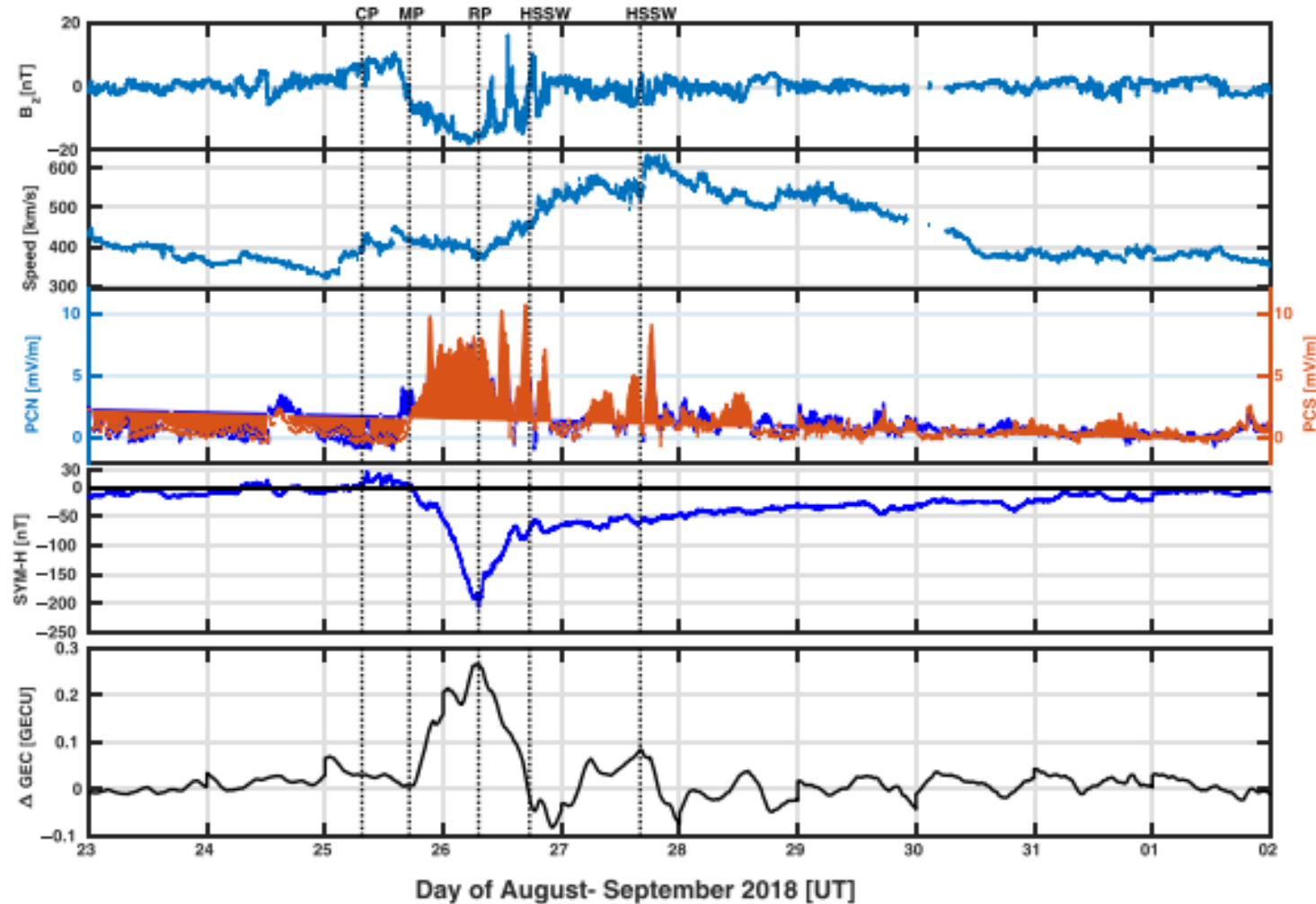
MAGNETIC STORM of St PATRICK'S DAY : MAPS of VTEC



Variations near the magnetic Equator due to a CME (~200 GPS stations)

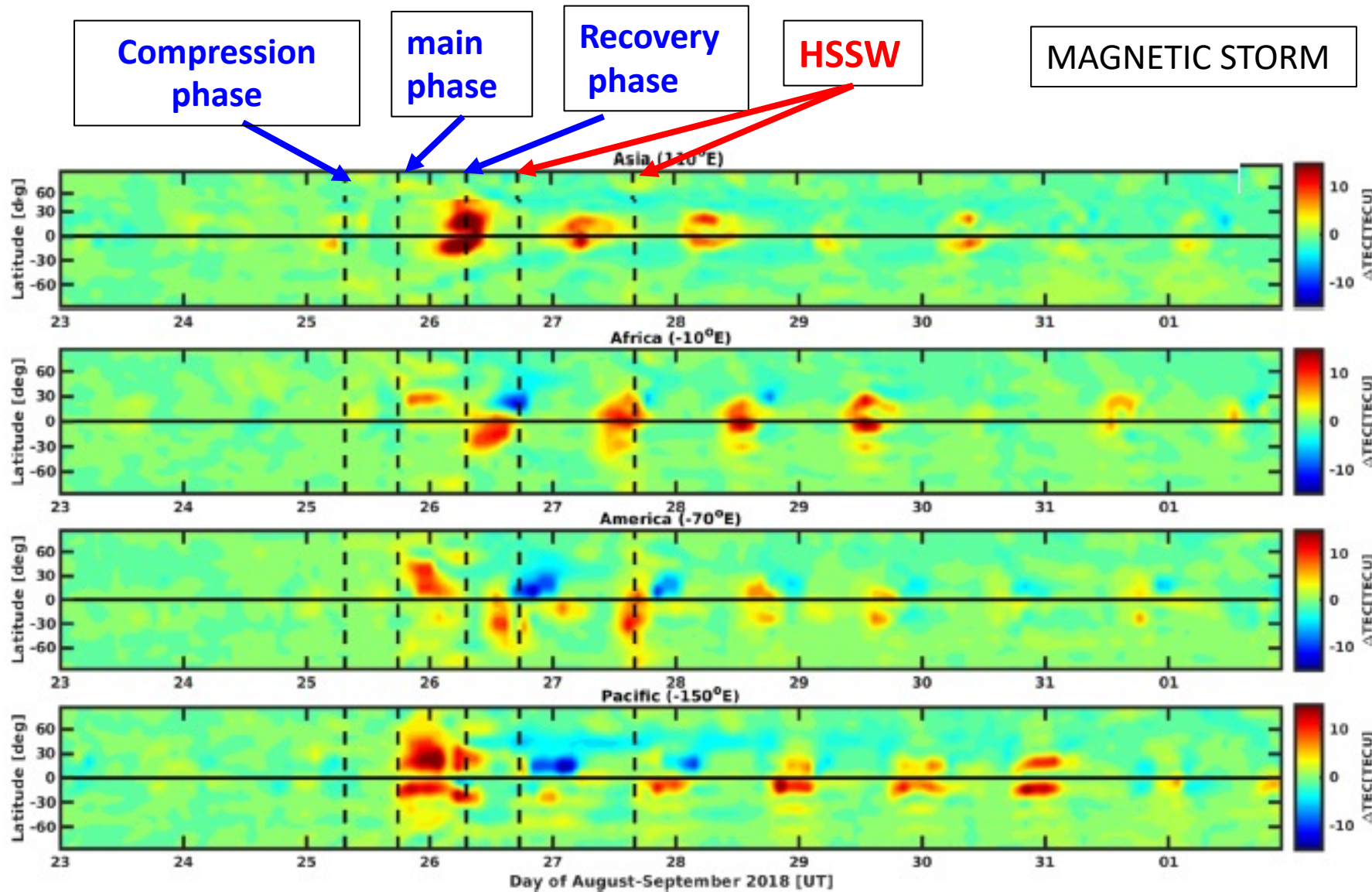
Nava,, et al., "Middle and low latitude ionosphere response to 2015 St. Patrick's Day geomagnetic storm", J. Geophys. Res. Space Physics,121, 3421–3438, doi:10.1002/ 2015JA022299.

Global parameters, from 23 August to 1 September: (from top to bottom) the Bz component of IMF in nanotesla, the solar wind speed in km/s, the SYM-H index in nanotesla, polar cap indices in mV/m, and GEC in GECU **[PAKISTAN]**



Younas, W. C., C. Amory-Mazaudier, M. Khan, R. Fleury, Ionospheric and Magnetic signatures of a Space Weather event on 25-29 August 2018 : CME and HSSWs, , Journal of Geophysical Research: Space Physics, 125, e2020JA027981.

<https://doi.org/10.1029/2020JA027981>



VTEC is influenced by PPEF, DDEF and Thermal expansion of atmosphere

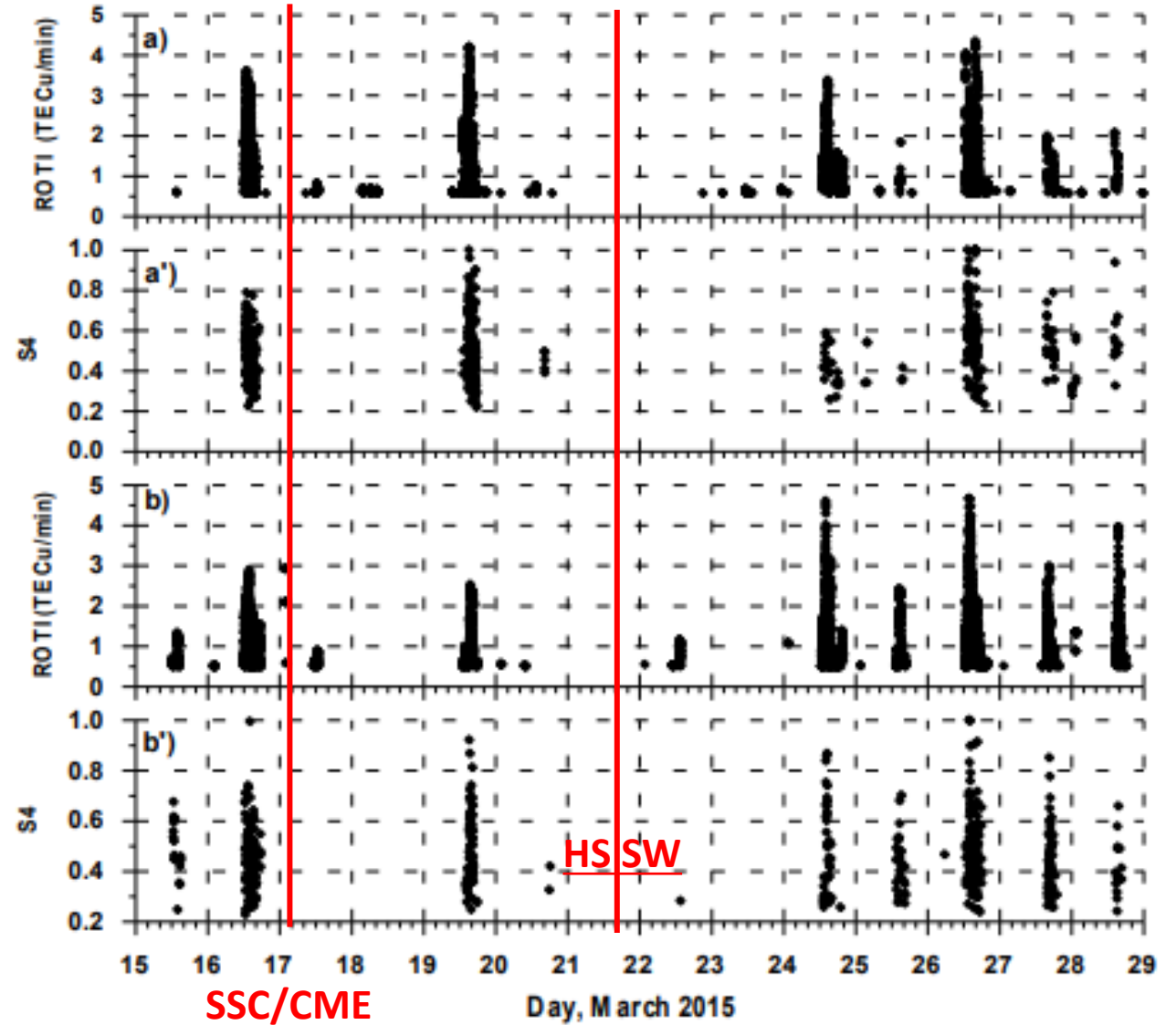
Younas,W et al., Journal of Geophysical Research, Space Physics, 125, e2020JA027981. <https://doi.org/10.1029/2020JA027981>

ROTI and S4 Indices

$$\text{rot} = \frac{STEC_{k+1} - STEC_k}{time_{k+1} - time_k} * 60$$

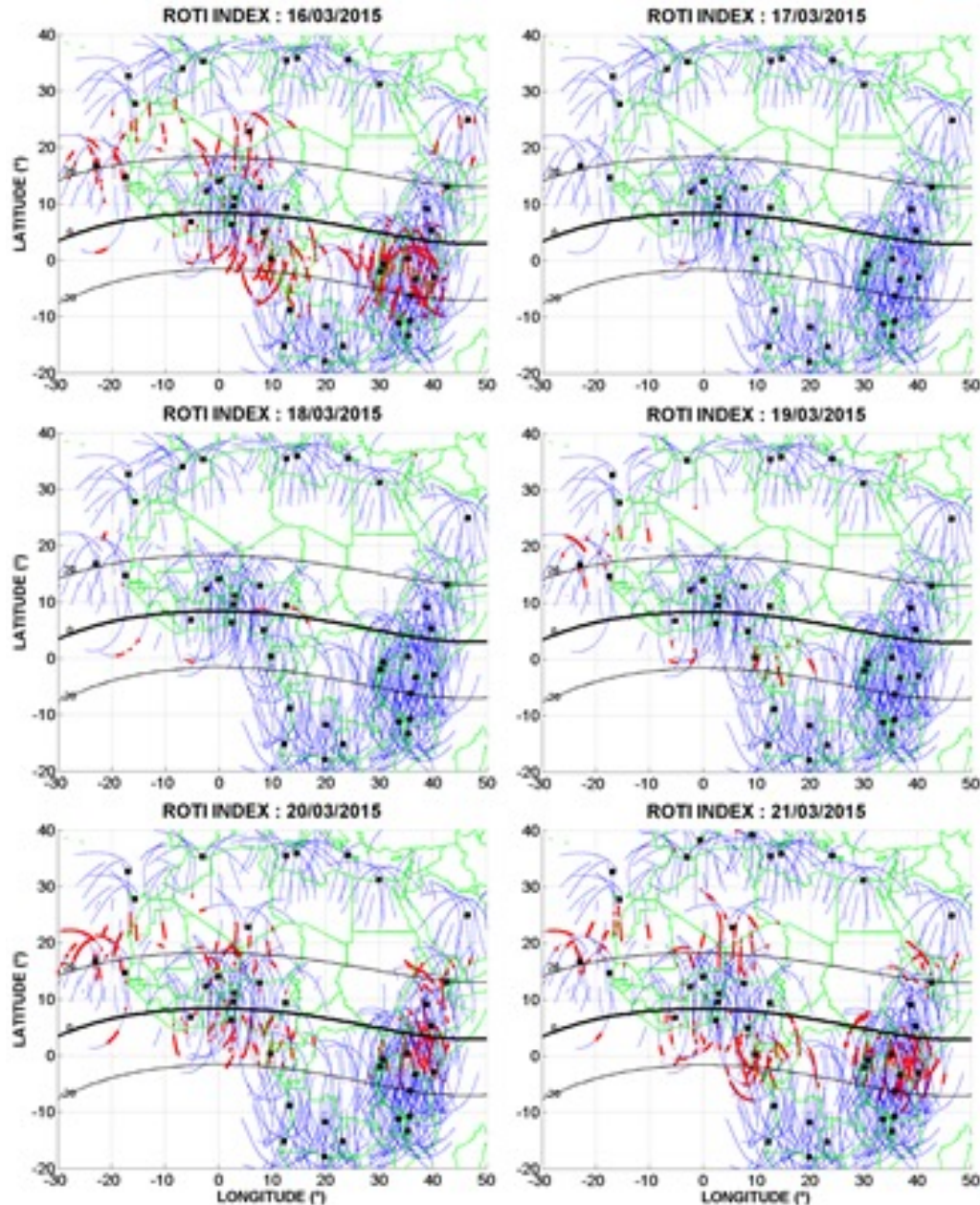
$$s4 = \sqrt{\frac{\langle I^2 \rangle - \langle I \rangle^2}{\langle I \rangle^2}} \quad I = \frac{A^2}{2}$$

I : intensity of the signal



Storm March 17, 2015 /equinox

Dst < -200 nT, storm started at 04.45 UT



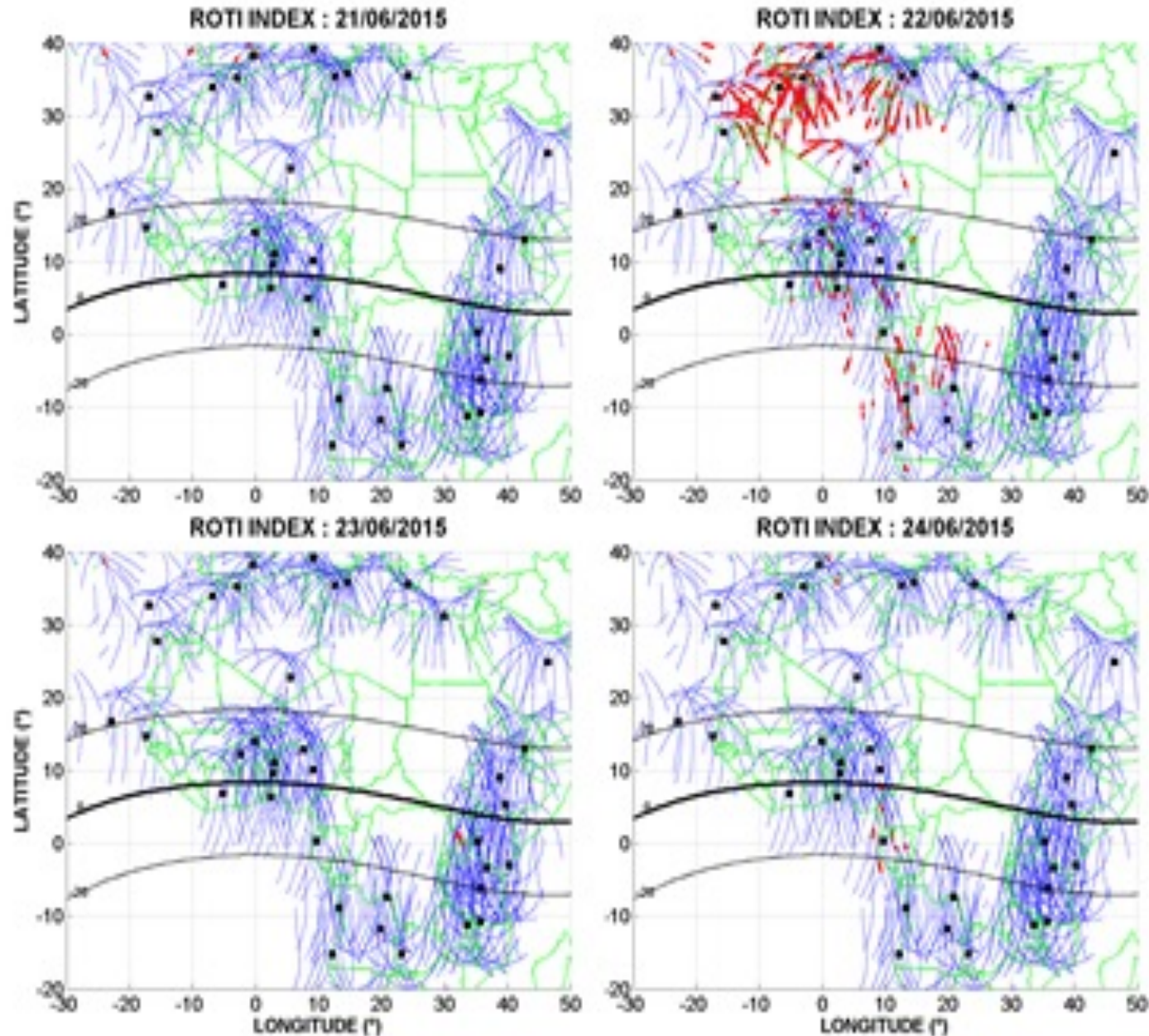
Rate of change of total electron content index (ROTI) maps over African region during St. Patrick's Day storm, 16–21 March 2015. Thin blue lines show ROTI ≤ 1.5 TECU/min, while red squares represent ROTI > 1.5 TECU/min. Black squares indicate Global Navigation Satellite System station used to produce ROTI maps

$$\text{rot} = \frac{STEC_{k+1} - STEC_k}{time_{k+1} - time_k} * 60$$

Inhibition of scintillations over the whole earth during several days : DDEF effect long duration

Kashcheyev, A., et al., "Multi-variable comprehensive analysis of two great geomagnetic storms of 2015", Journal of Geophysical Research: Space Physics, 123. <https://doi.org/10.1029/2017JA024900>

Storm June 22, 2015 solstice



$$\text{rot} = \frac{STEC_{k+1} - STEC_k}{\text{time}_{k+1} - \text{time}_k} * 60$$

Dst < -200 nT
Storm started at 18.33 UT, it is the time of the Pre reversal enhancement of the eastward electric field

Increase of scintillations
PPEF effect short duration

Disturbed magnetic field

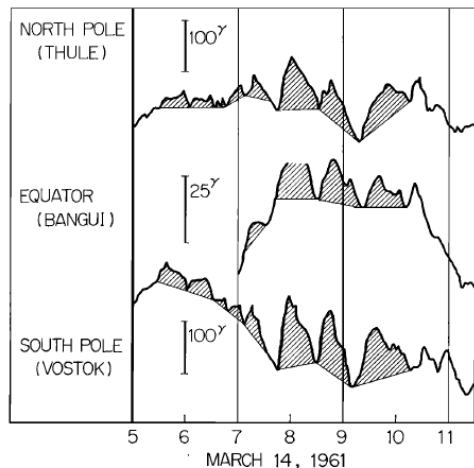


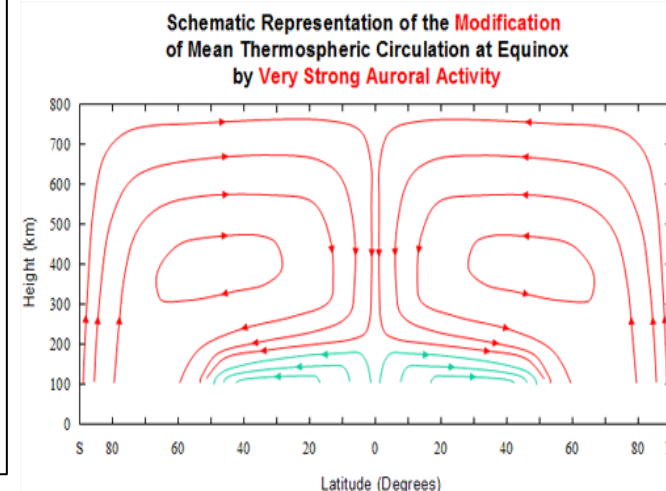
Fig. 1. Train of D_{st-2} fluctuations (shaded). Geomagnetic latitudes of these stations are 88.9 (Thule), 06.0 (Bangui), and -89.1 (Vostok).

Model of Fejer et al.,(2008)

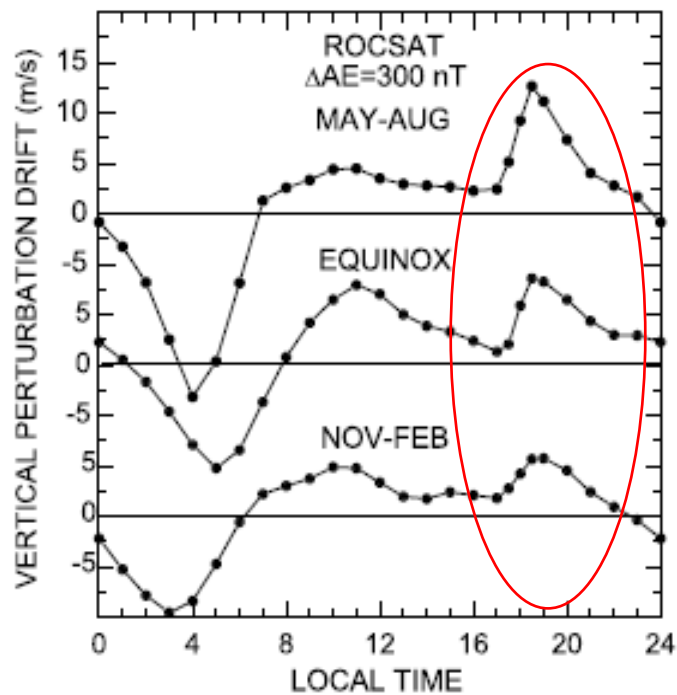
Geophysical Research Letters, 35, L20106.
<https://doi.org/10.1029/2008GL035584>

PPEF is an eastward E_y , **increases the PRE**
 DDEF is a westward E_y , **decreases the PRE**
 Eastward electric field => moves up
 Westward electric field => moves down

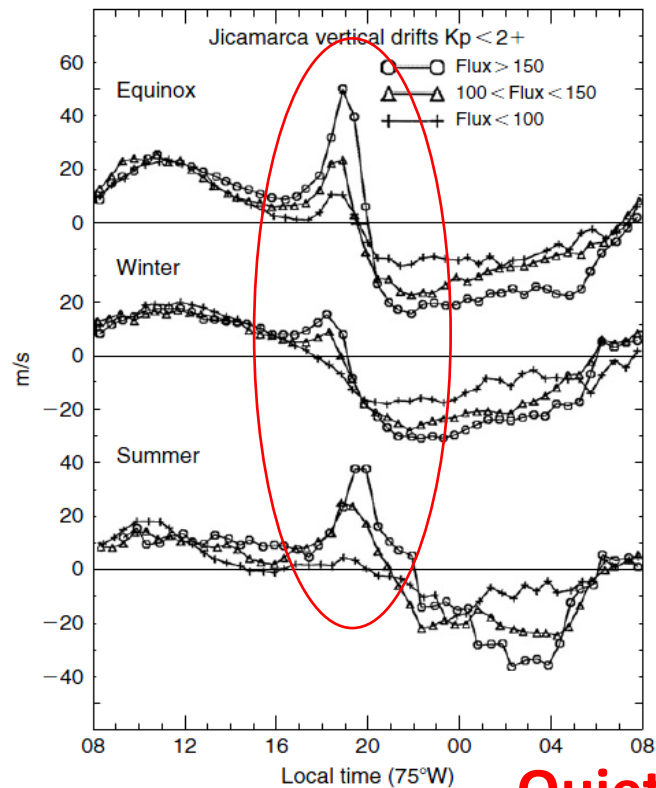
Disturbed thermospheric wind



PROMPT PENETRATION

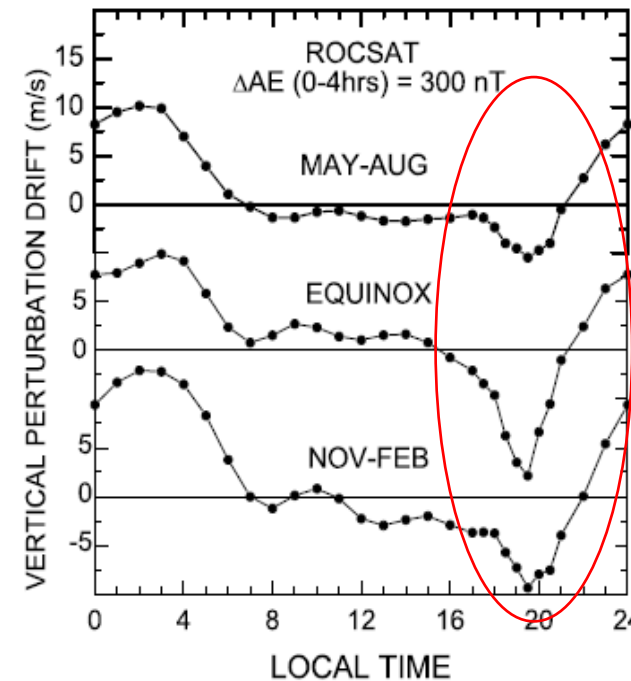


PPEF



Quiet day

DISTURBANCE DYNAMO



DDEF

Magnetic signatures [PPEF and DDEF]

Law of Biot and Savart

$$\Delta H = Sq + D_{iono} + D_{mag}$$

ΔH : H component of the Earth's magnetic field measured by magnetometers

Sq : regular variation of the Earth's magnetic field during magnetic quiet days

D_{iono} : magnetic disturbance due to the ionospheric electric currents

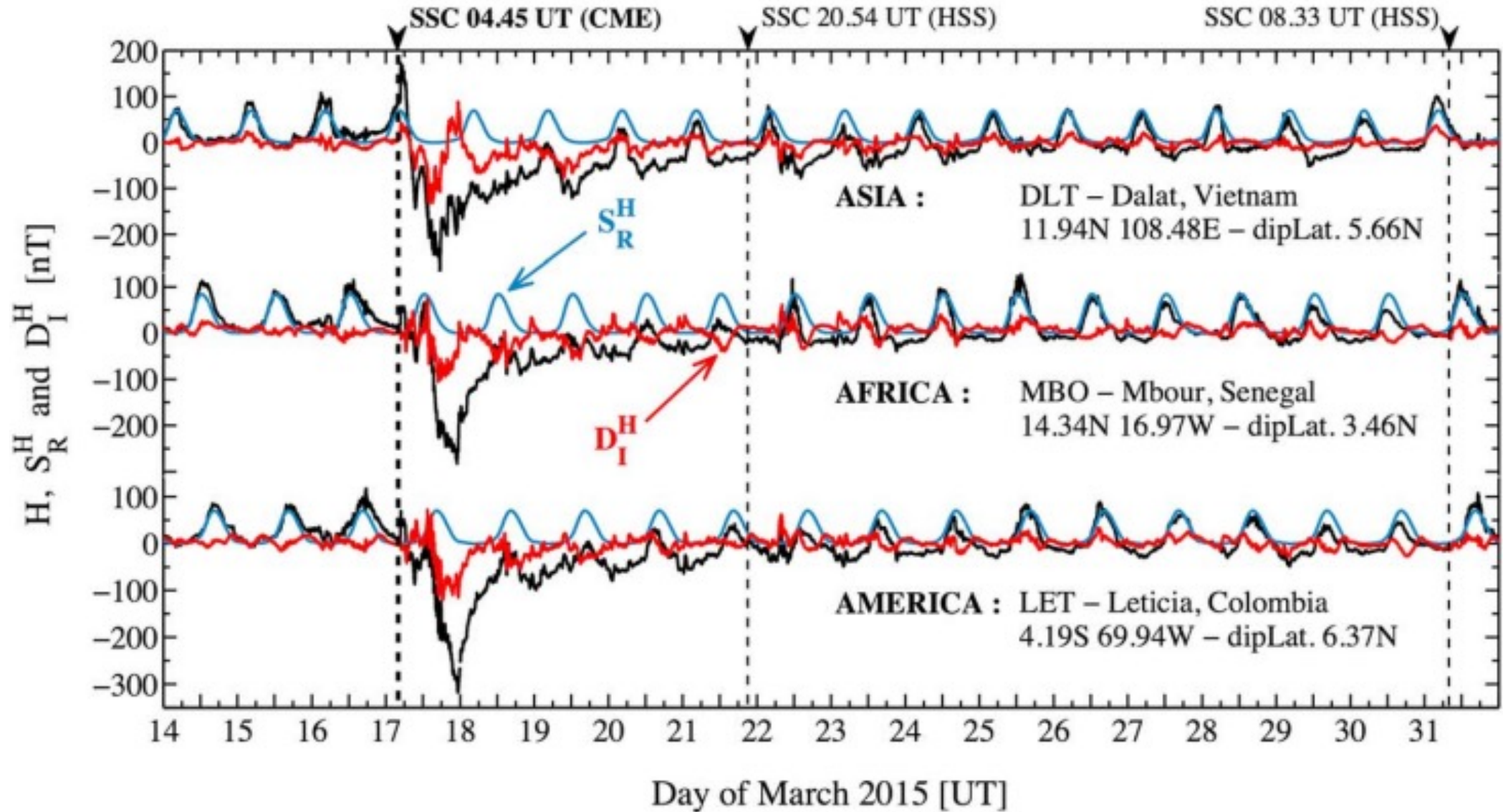
D_{mag} : magnetic disturbance due to the ionospheric electric currents (SYM-H, ASYM-H)

Disturbed ionospheric electric current

$$D_{iono} = \Delta H - Sq - D_{mag}$$

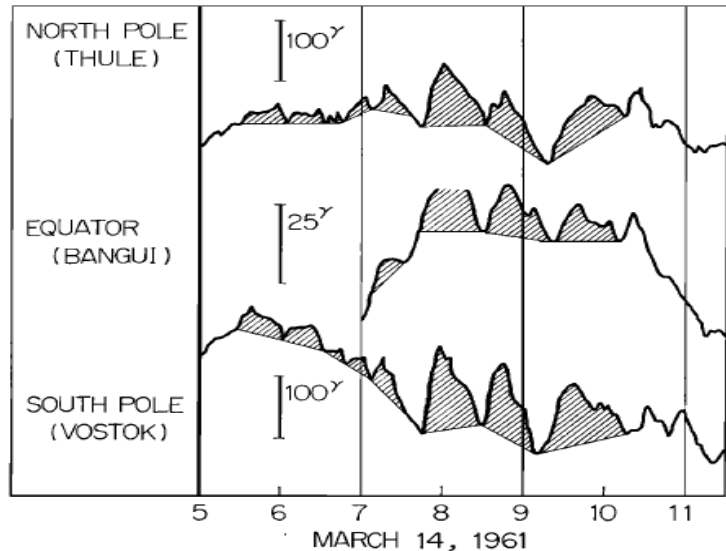
$$D_{iono} = DP_2 + D_{dyn}$$

H field component, H-quiet variation (S_R^H) and Disturbances (D_I^H)



blue : the Regular variation S_q , black : ΔH measured, red : Diono disturbance

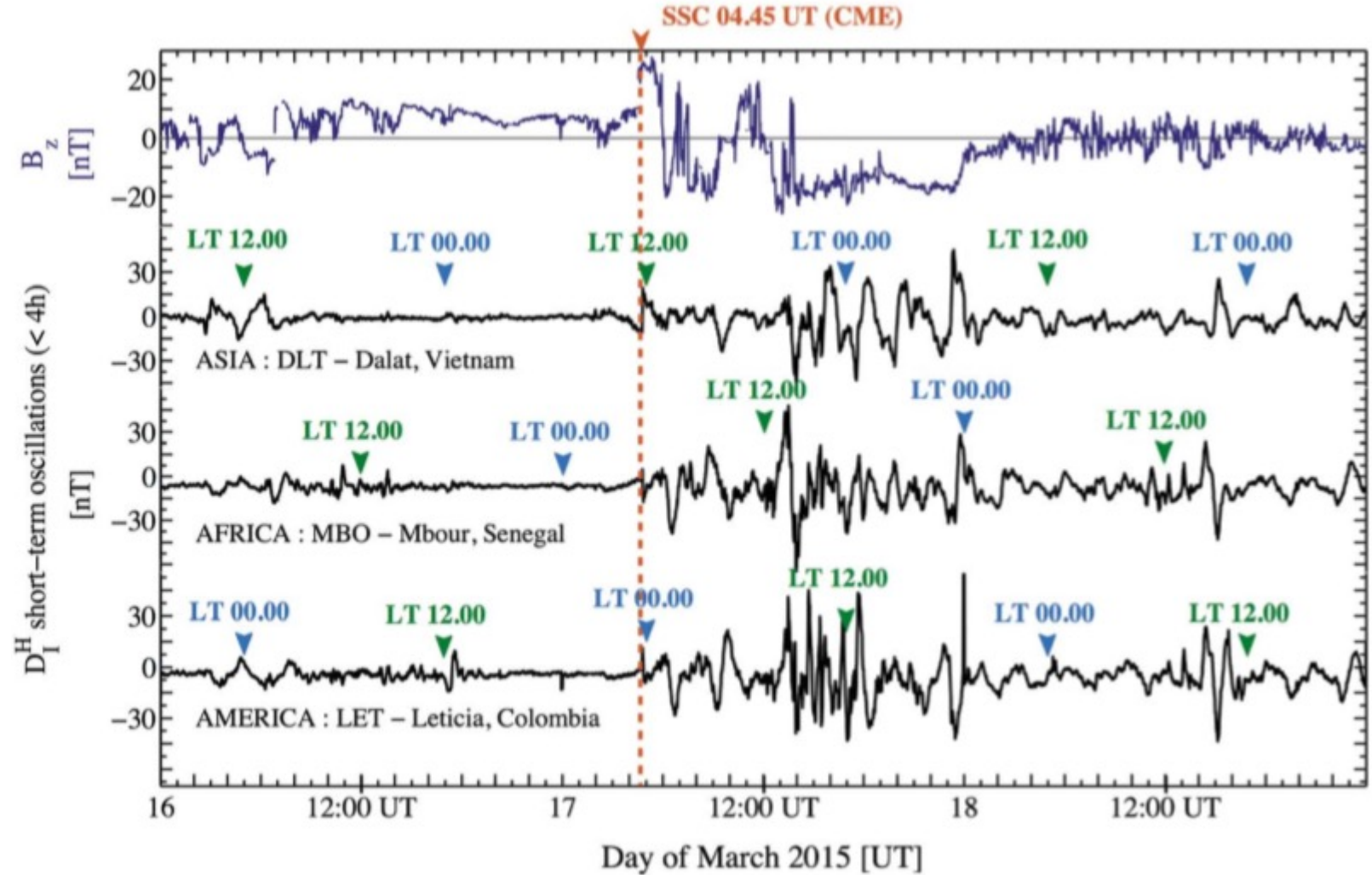
(Nishida, 1968)



Train of D_{st} fluctuations (shaded). Geomagnetic latitudes of these stations are (Thule), 05.0 (Bangui), and -89.1 (Vostok).

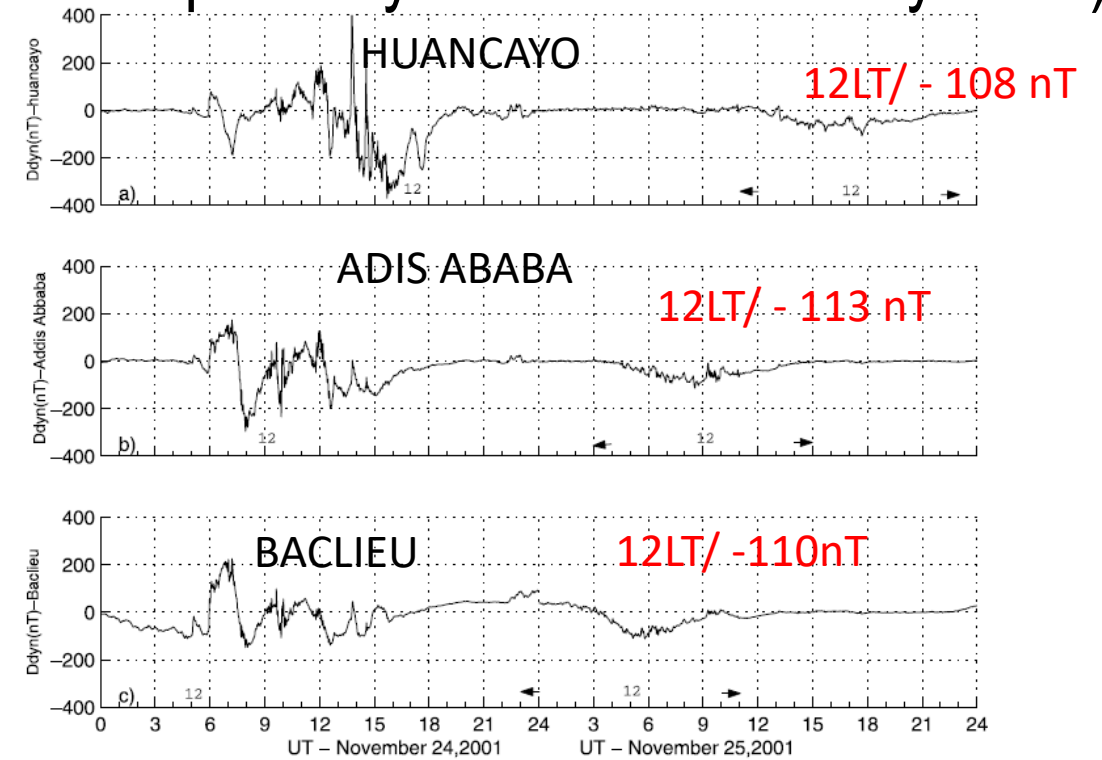
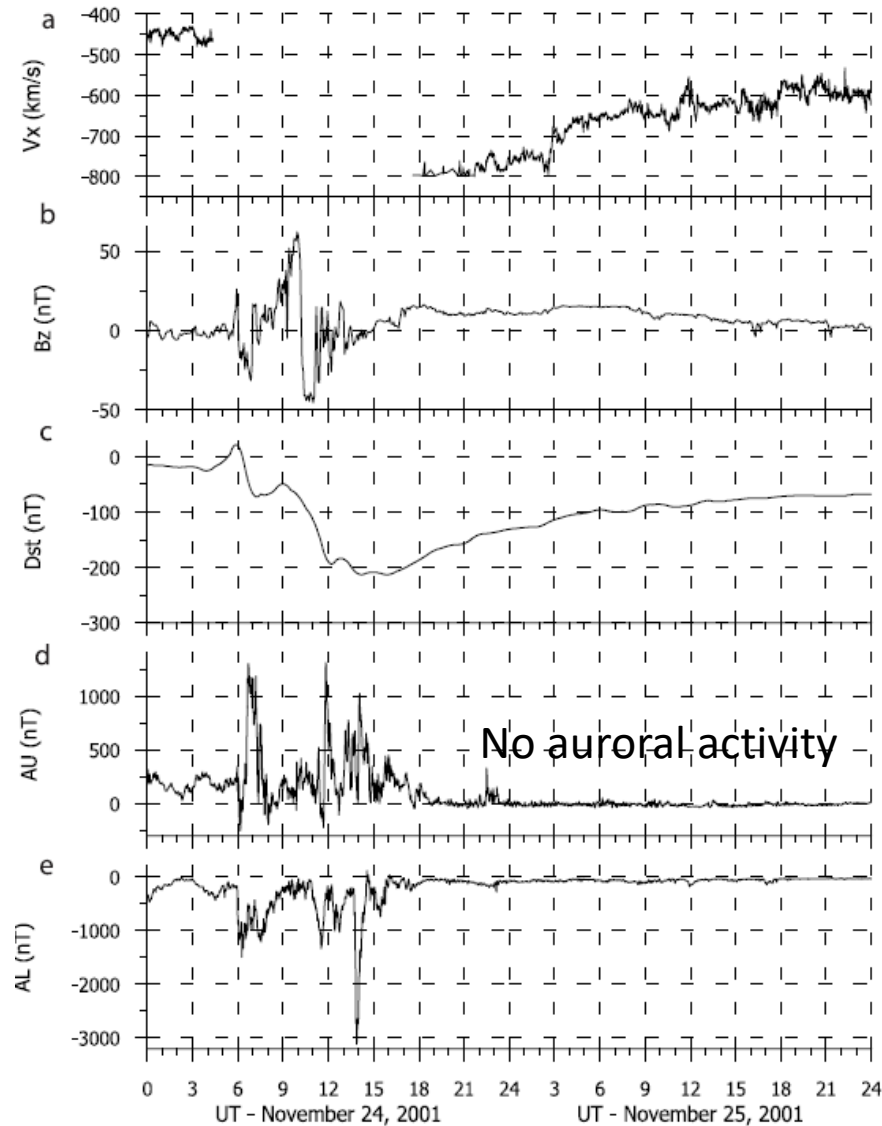
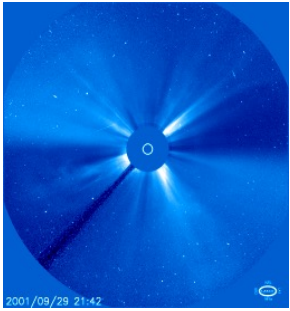
Magnetic signature of PPEF / DP₂

WORLD WIDE DISTURBANCE



Magnetic disturbance of the H component due to PPEF at specific longitudinal sectors, from 16 to 18 March, from top to bottom are plotted the B_z component of IMF, sectors. (Nava et al., JGR 2016)

Magnetic signature of DDEF D_{dyn} (simple case : a quiet day after a storm / only CME)



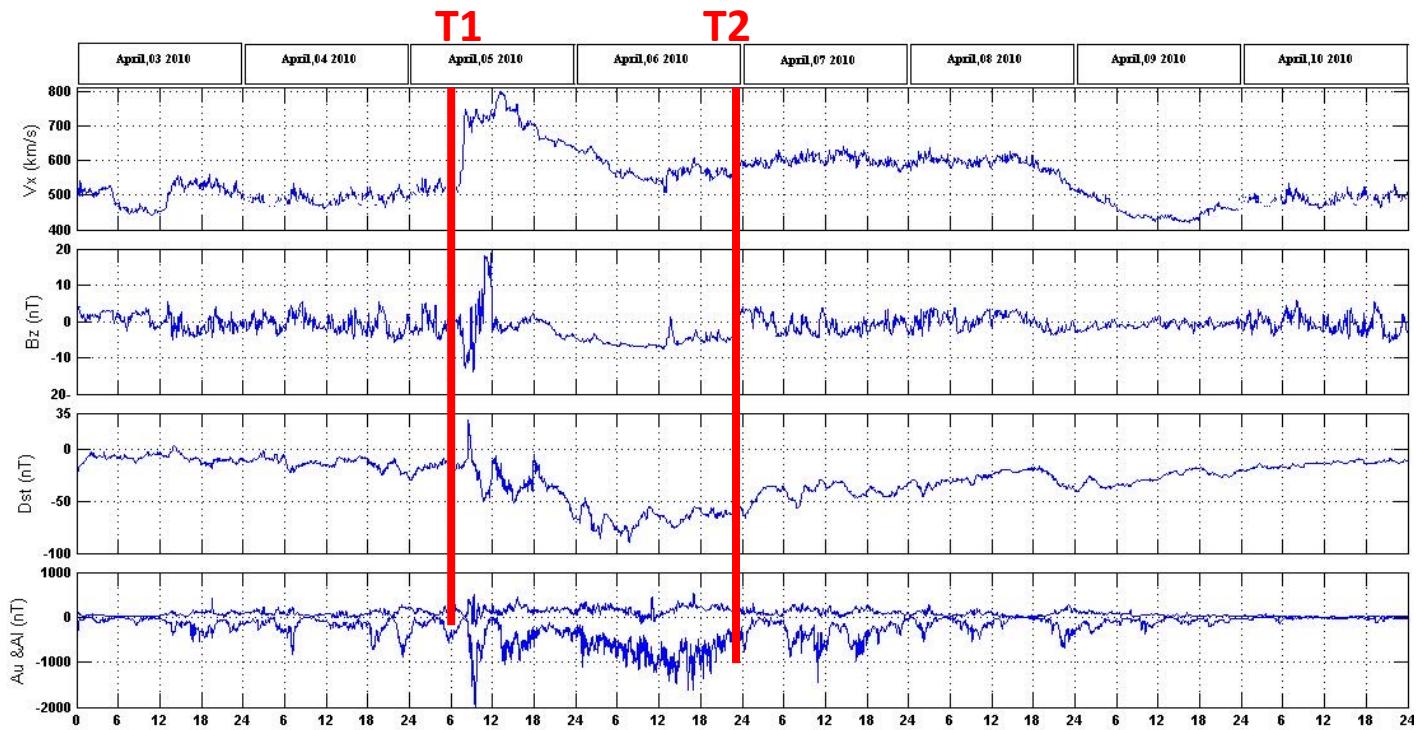
$$D_{iono} = DP_2 + D_{dyn}$$

To isolate the magnetic D_{dyn} due to the ionospheric disturbance dynamo at the equator, we selected magnetic quiet days just after the storm $\Rightarrow DP_2 \sim 0$

$$D_{iono} = D_{dyn}$$

Le Huy and Amory-Mazaudier, JGR 2005, 2008

Zaka et al., Annales Geophysicae 2009/ Zaka et al., JGR 2010 [modelling with TIEGCM]



T1 : Shock of CME on April 5 at 08h25

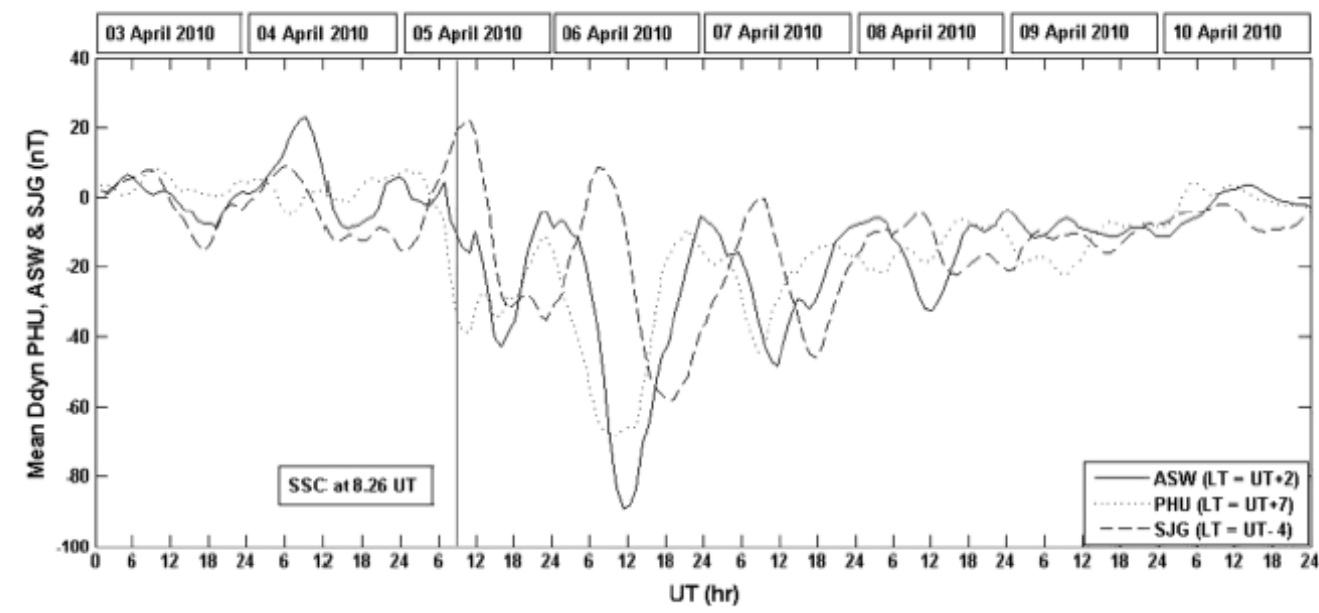
T2 : arrival of High Speed Solar Wind on April 6 around 24h00



To separate the effect of the DP2 signal from the disturbance dynamo (Ddyn) signal, **we take the average value of 4 h with sliding of 1 h for the whole period**

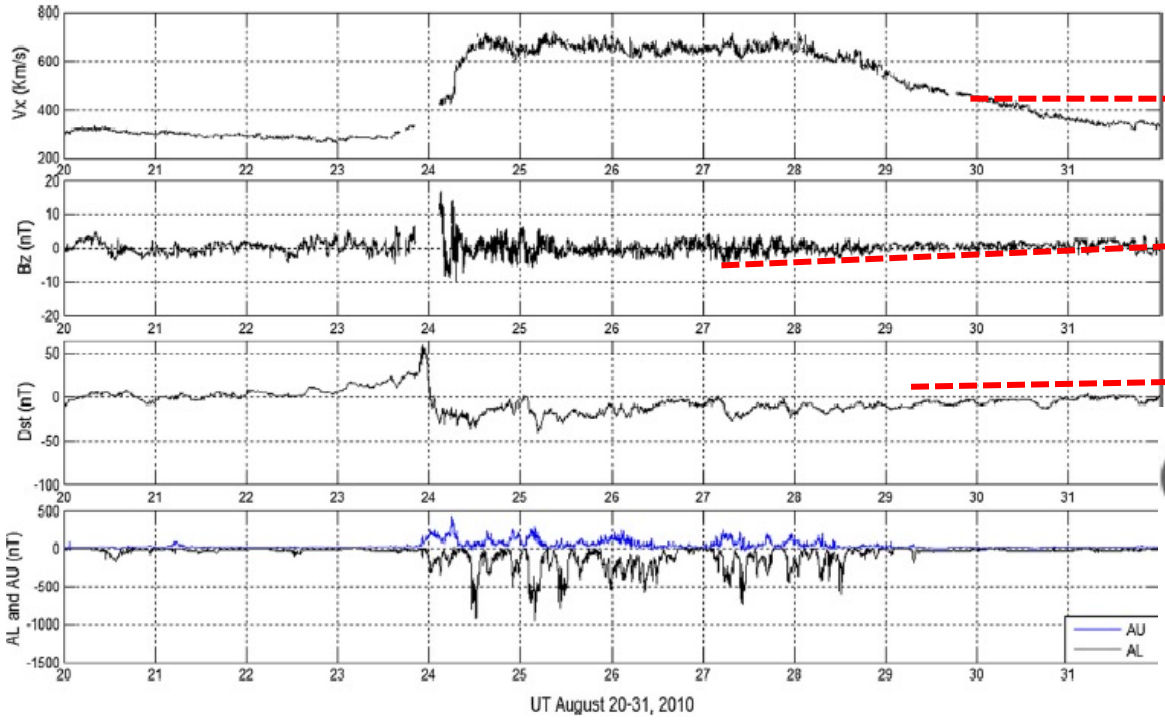
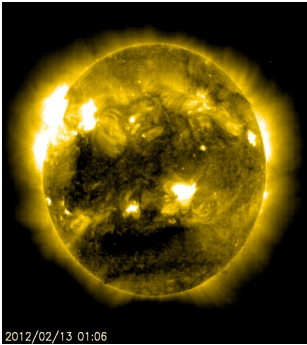
magnetic disturbance of DDEF, Ddyn, observed in the three longitude sectors : Asia, Africa , America , due to a CME followed by a high speed solar wind [April 2010],

Fathy, I., C. Amory-Mazaudier, A. Fathy, A. M. Mahrous, K. Yumoto, and E. Ghamry (2014), Ionospheric disturbance dynamo associated to a coronal hole: Case study of 5–10 April 2010, J. Geophys. Res. SpacePhysics, 119, 4120–4133, doi:10.1002/2013JA019510



HIGH SPEED SOLAR WIND

Features of HSSW

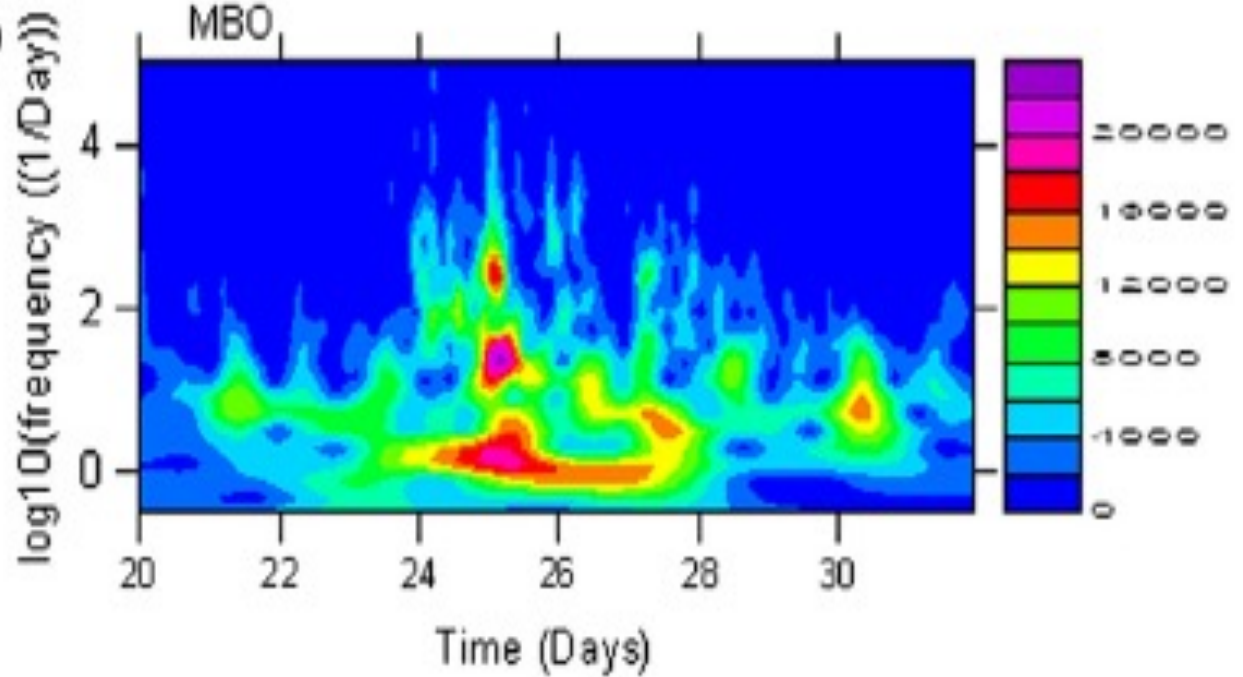


Large solar wind speed

Oscillating Bz

No large Dst

(b)



Scalograms revealing the amplitude **wavelet coefficients** of D_{iono} at MBO

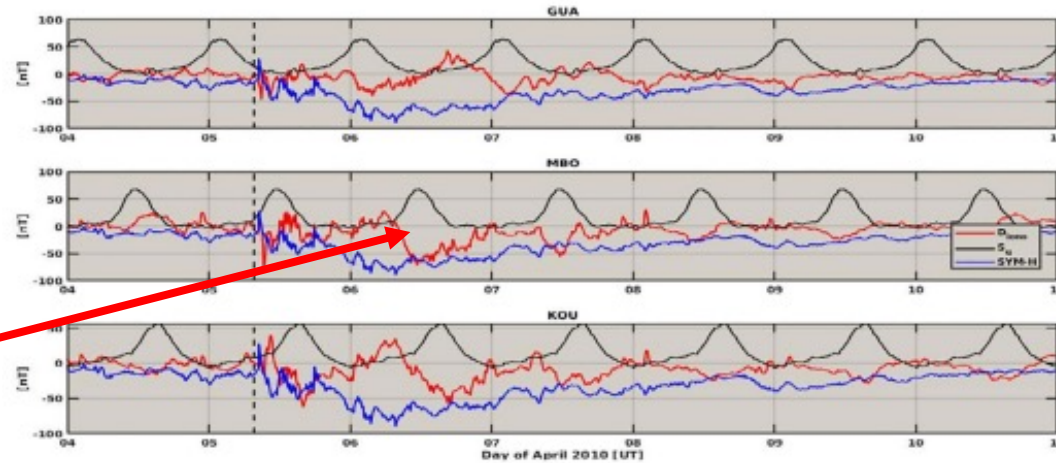
Zaourar, N., C. Amory-Mazaudier and R. Fleury, Hemispheric asymmetries in the ionosphere response observed during the high-speed solar wind streams of the 24-28 August 2010 (2017), Advances in Space Research, doi.org/10.1016/j.asr.2017.01.048.

Magnetic variations at three observatories located in three regions (from top to bottom): GUA (Asia), MBO (Africa), and KOU (America) from April 4-10, 2010. / **Law of Biot and Savart** /

$$\text{Disturbed ionospheric current } D_{\text{iono}} = \Delta H - S_q - D_{\text{mag}}$$

Top figure

ΔH measured (black),
Regular S_q variation (blue)
 $D_{\text{iono}} = DP_2 + D_{\text{dyn}}$ (red)



ASIA/GUA

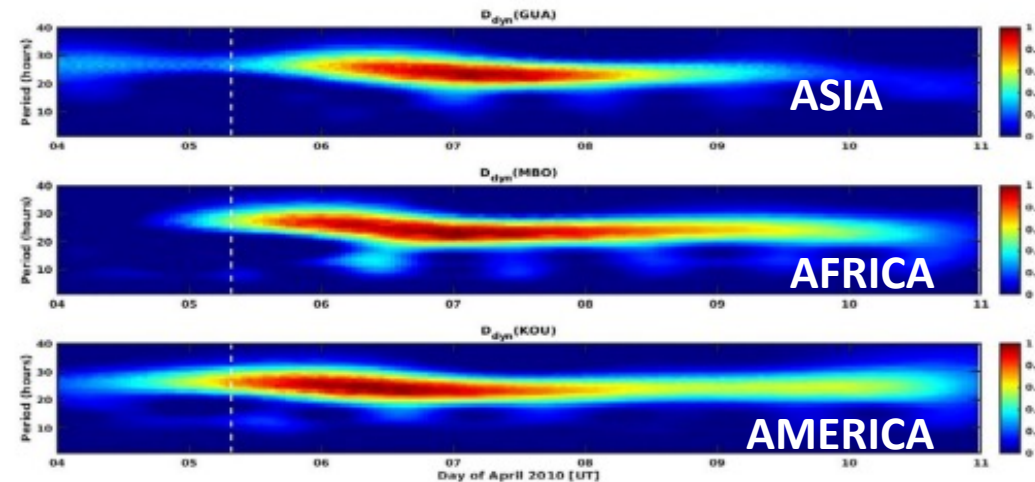
AFRICA/MBO

AMERICA/KOU

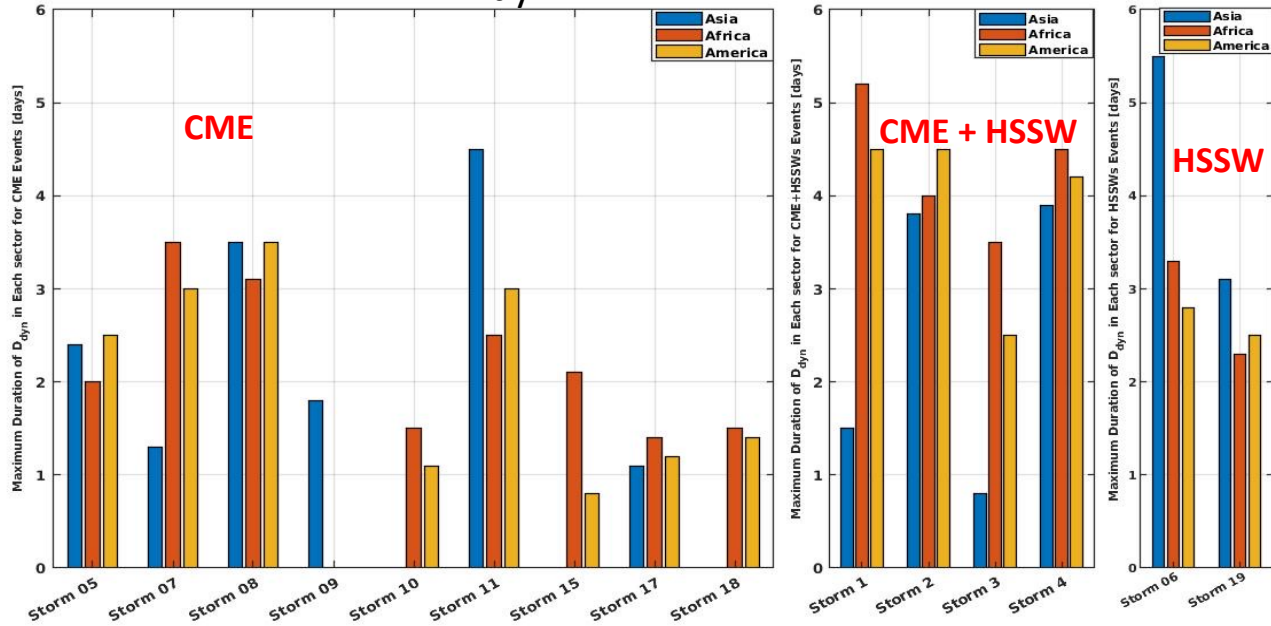
reversed from their observed normal quiet-day variation.

Bottom figure

Disturbance dynamo (D_{dyn}) estimated using **wavelet based semblance analysis**. The vertical dashed line corresponds to the arrival of CME

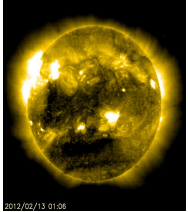
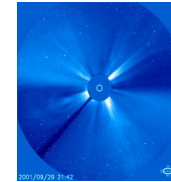


D_{dyn} DURATION

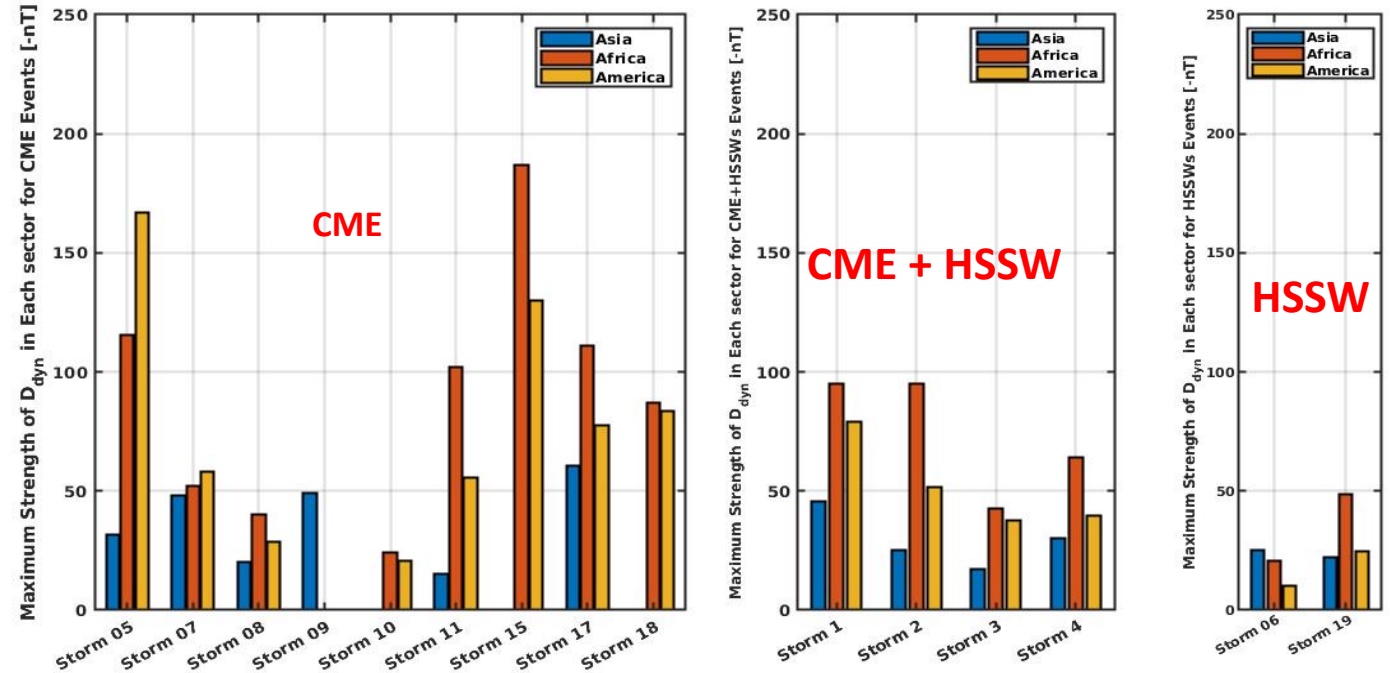


STUDY OF 19 STORMS

D_{dyn} Magnetic signature of DDEF



D_{dyn} STRENGTH



- *Longest duration for HSSW
- *Greater strength for CME
- *HSSW => All longitude sectors are disrupted
- *CME => 1, 2 or all longitude sectors disturbed

Younas, W. et al., Magnetic signatures of ionospheric disturbance dynamo for CME and HSSWs generated storms, Earth and Space Science, <https://doi.org/10.1029/2021SW002825>

Conclusion

The results presented concerns some direct impacts of Sun on the Earth.

It is a tiny part of space weather concerning certain relations between the Sun and the Earth. We have shown results obtained mainly with GNSS receivers and magnetometers. There are many other works using satellite data and models (IRI NeQuick, TIEGCM,

Studies are currently being developed on the effect of earthquakes, stratospheric warming or QBO on the variations of the Ionosphere, and GNSS receivers are again very useful.

There are a lot of data sets on the web, and this give opportunity to many students to do PhD and contribute to built this new systemic approach of the Sun Earth system needed for Space Weather.

The GNSS receivers can be also used to study the motions tectonic plates, the vapor water in the troposphere.